Paleobiology, 44(3), 2018, pp. 460–489
DOI: 10.1017/pab.2018.16

PALEOBIOLOGY
A PUBLICATION OF THE Paleontological SOCIETY

Blooms of aberrant planktic foraminifera across the K/Pg boundary in the Western Tethys: causes and evolutionary implications

Ignacio Arenillas, José A. Arz, and Vicente Gilabert

Abstract.—We report a detailed study of the different categories and types of abnormal morphologies in planktic foraminifera recognizable in the lowermost Danian, mainly from the El Kef and Aïn Settara sections, Tunisia. Various types of abnormalities in the test morphology were identified, including protuberances near the proloculus, abnormal chambers, double or twinned ultimate chambers, multiple ultimate chambers, abnormal apertures, distortion in test coiling, morphologically abnormal tests, attached twins or double tests, and general monstrosities. Detailed biostratigraphic and quantitative studies of the Tunisian sections documented a major proliferation of aberrant planktic foraminifera (between approximately 5% and 18% in relative abundance) during the first 200 Kyr of the Danian, starting immediately after the Cretaceous/Paleogene (K/Pg) boundary mass extinction (spanning from the *Guembelitria cretacea* Zone to the lower part of the *P. pseudobulloides* Zone). This contrasts with the proportionately low frequency of aberrant tests (generally <2%) identified within the uppermost Maastrichtian, suggesting more stable environmental conditions during the last ~50–100 Kyr of the Cretaceous. Two main pulses with abundant aberrant tests were recognized in the earliest Danian, the one recorded in the well-known K/Pg boundary clay being the more intense of those (maxima of >18%). These main pulses of aberrants coincide approximately with relevant quantitative and evolutionary turnovers in the planktic foraminiferal assemblages. In this paper, we explore the relation of these high values of the foraminiferal abnormality index with the environmental changes induced by the meteorite impact of Chicxulub in Yucatan, Mexico, and the massive eruptions of the Deccan Traps, India.

Ignacio Arenillas, José A. Arz, and Vicente Gilabert. Departamento de Ciencias de la Tierra and Instituto Universitario de Investigación en Ciencias Ambientales de Aragón, Universidad de Zaragoza, E-50009, Spain. E-mail: ias@unizar.es

Accepted: 3 April 2018
Published online: 13 July 2018
Data available from the Dryad Digital Repository: https://doi.org/10.5061/dryad.n1q6527

Introduction

Asteroid impacts represent an extreme among natural disasters, inducing rapid and sharp environmental perturbations with important implications for the biosphere (Alvarez et al. 1992; Toon et al. 1997). After the Chicxulub asteroid impact (Yucatan, Mexico) at the Cretaceous/Paleogene (K/Pg) boundary (Hildebrand et al. 1991), a cloud of dust and fine ejecta scattered and contaminated the atmosphere, land, and oceans (Alvarez et al. 1980; Smit and Hertogen 1980). The cloud of pulverized impact material at Chicxulub was deposited slowly (probably over a few years), forming a thin (few millimeters) airfall layer evident in deep-marine sediments worldwide, with anomalous concentrations of iridium and other platinum-group metals, nickel-rich spinels, shocked quartz, and altered microtektites (Smit 1990; Robin et al. 1991). The Chicxulub impact caused the blockage of sunlight, the inhibition of the photosynthesis, disruption of food chains, a sudden drop in global temperature, destruction of the ozone layer, and the production of toxins and acid rain (Smit and Romein 1985; Hsü and McKenzie 1985; Pope et al. 1997; Gerasimov 2002; Ocampo et al. 2006; Alegret et al. 2012; Bardeen et al. 2017), initiating one of the greatest mass extinctions in the history of life (Schulte et al. 2010).

In the earliest Danian oceans, a dark-clay bed was deposited above the K/Pg airfall layer under conditions of global climatic warming and alterations in oceanic productivity (Hsü and McKenzie 1985; D'Hondt et al. 1998; D'Hondt 2005; Coxall et al. 2006; Birch et al. 2016), with some regions showing a sharp decline in export productivity during approximately 2 Myr, and others a constant or rapidly reestablished

0094-8373/17

organic flux from the surface ocean to the deep seafloor (Hull and Norris 2011).

The dark-clay bed also contains high concentrations of heavy metals, which, though lower than in the airfall layer, are higher than in the sediments of the upper Maastrichtian and more modern lower Danian (Smit and ten Kate 1982; Dupuis et al. 2001; Hollis et al. 2003). The paleoenvironmental conditions recorded in the dark-clay bed seem therefore to reflect the long-term disruptive effects of the K/Pg impact event, revealing a time in which the ecosystems were starting to recover and oceanic productivity to re-establish itself.

Planktic foraminifera, like other paleontological groups, suffered considerable, but not complete, extinction at the K/Pg boundary event (Smit 1982). The cause–effect relationship between the Chicxulub impact and the K/Pg mass extinction has been amply verified (see Smit 1990, 1999; Arenillas et al. 2000b, 2006), and the impact theory is correspondingly well established in the scientific community (Schulte et al. 2010). However, other evidence seems to suggest that the massive eruptions of the Deccan Traps, India, could have played an important role in the extinction, or at least in the paleoenvironmental changes that occurred during the Cretaceous/Paleogene transition (Courtillot et al. 1988; Chenet et al. 2007, 2009; Keller et al. 2011, among others). Recently, Schoene et al. (2015) has applied uranium-lead (U-Pb) zircon geochronology to Deccan rocks, showing three main eruptive phases or megapulses, the main one (phase 2) beginning approximately 250 Kyr before K/Pg boundary and lasting 750 Kyr.

The Deccan megapulses have been related to episodes of global warming and/or environmental stress across the K/Pg boundary (Keller and Pardo 2004; Pardo and Keller 2008; Punekar et al. 2014, 2016). Keller et al. (2011) proposed that phase 2 (responsible for ca. 80% of the total volume of Deccan Traps emissions) ended at or near the K/Pg boundary, spanning the last 280 Kyr of the Maastrichtian. Deccan-induced global warming and cooling episodes at the late Maastrichtian seem to be responsible for dwarfing episodes in some planktic foraminiferal species (Keller and Abramovich 2009; Omaña et al. 2012; Petersen et al. 2016), migrations (Olsson et al. 2001), and regional assemblage changes (Keller 2003), however, without a significant decrease in global planktic foraminiferal diversity (Arenillas et al. 2000a,b). After the K/Pg boundary, small species began to appear following a model of "explosive" adaptive radiation (Smit 1982; Brinkhuis and Zachariasse 1988; Arenillas et al. 2002, 2004). One of the ancestors of the first Danian species was the opportunistic, triserial genus *Guembelitria*, which might be the only true survivor (Smit 1982, 2004). However, the main lineages of planktic foraminifers appearing in the Danian, whose descendants have reached the present day, could have a benthic origin (see Brinkhuis and Zachariasse 1988; Arenillas and Arz 2017). It must be emphasized that there are other relevant taxonomic and phylogenetic models, some of them highly supported among planktic foraminifer taxonomists. Among the most noteworthy proposals are those of Olsson et al. (1999), Apellaniz et al. (2002), Aze et al. (2011), and Koutsoukos (2014), which suggest that the genus *Muricohedbergella* was a survivor of the K/Pg extinction event and played an important phylogeny role for being the ancestral form of Danian genera such as *Globanomalina*, *Eoglobigerina*, and/or *Praemurica*.

Abnormal tests have long been reported in recent benthic foraminifera linked to regions with either high environmental variability (e.g., Polovodova and Schonfeld 2008; Ballent and Carignano 2008) or human-induced pollution (e.g., Yanko et al. 1998; Samir and El Din 2001; Frontalini and Coccioni 2008), showing that abnormal variations in morphology are a response to changes in ecological parameters such as temperature, pollution, carbonate solubility, dissolved oxygen, or the occurrence of rapid environmental fluctuations. The long-term effects of Chicxulub impact and the Deccan eruptions probably triggered similar ecological stress conditions, thus inducing similar malformations in planktic foraminiferal tests. Indeed, abnormal planktic foraminifers have been reported right above the K/Pg boundary, mainly in *Guembelitria* (Coccioni and Luciani 2006). Similar increases in abnormal planktic tests have been observed in warming episodes and episodes of ecological stress, such as the Cretaceous ocean anoxic events (Verga and Premoli Silva 2002) or the Paleocene–Eocene

https://doi.org/10.1017/pab.2018.16 Published online by Cambridge University Press

Thermal Maximum (Luciani et al. 2007). However, studies on the aberrant planktic foraminifers of the K/Pg transition from a taxonomic and paleoenvironmental point of view are still very limited and fragmented.

Abnormalities are formed when the ontogenetic plan of the test is disrupted and this disruption generates an irregular shape in comparison with other specimens of the same species (Murray 2006). In recent foraminifera, abnormalities produced during the life and growth of an individual may be due either to mechanical or ecological causes (Boltovskoy and Wright 1976; Murray 2006). In the case of planktic foraminifera, the causes behind test abnormalities may be predation breakages, but abnormal planktic specimens seem to reflect mainly stressful environmental conditions (Montgomery, 1990; Luciani et al. 2007). In addition, abnormalities can also be produced by mutations. The phenotypic consequences of mutations can vary, but in the case of fossil foraminifera, the most interesting ones are those that affect the test morphology. Mutations can cause lethal or physiologically nonfeasible aberrations, but could have also generated new species, probably bringing on the early Danian evolutionary radiation mentioned earlier (Bou-Dagher-Fadel 2012; Arenillas et al. 2016).

In this paper, a wide variety of morphological abnormalities in planktic foraminiferal tests from the earliest Danian are described for the first time, mainly from Tunisian sections. We use a quantitative approach to identify changes in the abundance of aberrant tests and correlate them with evolutionary radiations and other shifts recognized in the planktic foraminiferal assemblages across the K/Pg boundary. The main aim is to inquire into the causes that could have triggered the proliferation of aberrant tests before and after the K/Pg boundary mass extinction, and the relation of these causes with the environmental changes induced by the Deccan eruptions and the Chicxulub impact.

Material and Methods

Geological Context and Micropaleontological Sampling.—We studied samples from localities considered to be the most expanded and continuous marine K/Pg sections worldwide, such as El Kef, Aïn Settara, and Elles (Tunisia), and Agost and Caravaca (Spain). The El Kef section was chosen to define the Global Boundary Stratotype Section and Point (GSSP) for the base of the Danian stage, or the K/Pg boundary (Molina et al. 2006), while Caravaca, Elles, and Aïn Settara were chosen as auxiliary sections of the GSSP (Molina et al. 2009). The K/Pg boundary is defined at the base of the bed informally known as the "K/Pg boundary clay," specifically at the base of the 2- to 5-mm-thick airfall layer with high concentrations of iridium that coincides with the planktic foraminiferal extinction horizon (Smit 1990, 1999). The dark-clay bed overlying the K/Pg airfall layer is approximately 100 cm thick in El Kef, with a 50-cm-thick blackish clay overlain by a 50-cm-thick dark gray clay; it continues with 1-m-thick darkened gray marly clay and 60-cm-thick clayey marl, so the dark-clay bed thickness could be 200 cm or more in El Kef. It is characterized by low values of $\delta^{13}C$ and $CaCO_3$ content and high total organic carbon (TOC) values (Keller and Lindinger 1989). In Aïn Settara, the airfall layer is 5 to 10 mm thick, and the dark-clay bed is approximately 50 cm thick; this is also characterized by low values of $\delta^{13}C$ and in $CaCO_3$ content and high TOC values (Dupuis et al. 2001).

For the taxonomic studies, specimens were picked mainly from El Kef and Aïn Settara, where the foraminiferal test preservation is good (excellent at some samples), although specimens from other sections (Elles, Agost, and Caravaca) were used with the aim of conveniently illustrating some of the species and types of normal and abnormal growth morphologies identified in the lower Danian. Specimens considered to be normal forms are those that conform to some type of shape within the theoretical three-dimensional morphospace of serial and spiral foraminifeal tests proposed by Tyszka (2006). Taxonomic remarks and a systematic scheme for the normal forms of early Danian planktic foraminiferal species are provided in Supplementary Appendix A and Supplementary Figure 1.

All rock samples studied were disaggregated in water with diluted H_2O_2,

https://doi.org/10.1017/pab.2018.16 Published online by Cambridge University Press

washed through a 63 μm sieve, and then oven-dried at 50°C. The quantitative analyses were based on representative splits (using a modified Otto microsplitter) of approximately 300 specimens per sample, quantifying the relative abundance of both normal and abnormal tests in each group of planktic foraminifera (Tables 1, 2). For the quantitative study, we restudied 39 samples from El Kef and 35 samples from Aïn Settara (see Arenillas et al. 2000a, b). The specimens analyzed were mounted on microslides for a permanent record and identification. Planktic foraminifera were picked from the residues and selected for scanning electron microscopy (SEM), using the JEOL JSM 6400 and Zeiss MERLIN FE-SEM of the Electron Microscopy Service of the Universidad de Zaragoza (Spain). SEM photographs of the species considered here are provided in Supplementary Figures 2 and 3. For the illustration of these species, we used, in addition to El Kef and Aïn Settara, other localities characterized by the good preservation of their foraminiferal tests, such as Ben Gurion (Israel), Deep Sea Drilling Project (DSDP) Site 305 (North Pacific), and Bajada del Jagüel (Argentina).

Planktic Foraminiferal Biochronology.—For the Maastrichtian, the biostratigraphic and quantitative study focused mainly on the *Plummerita hantkeninoides* Subzone, which spans the last 140 Kyr of the Cretaceous according to Husson et al. (2014). This biozone is defined by the total range of the nominate taxon and is equivalent to the alphanumeric Zone CF1 of Li and Keller (1998). For the lower Danian, we used the biozonation of Arenillas et al. (2004), and compared it with those of Li and Keller (1998) and Berggren and Pearson (2005) (the latter recently revised by Wade et al. 2011). Their equivalences are shown in Figure 1. The former is based on continuous, complete, and very expanded Tunisian and Spanish K/Pg sections such as El Kef, Aïn Settara, Elles, Caravaca, Agost, and Zumaia. It includes six subbiozones: the *Muricohedbergella holmdelensis* and *Parvularugoglobigerina longiapertura* Subzones of the *Guembelitria cretacea* Zone, the *Parvularugoglobigerina sabina* and *Eoglobigerina simplicissima* Subzones of the *Pv. eugubina* Zone, and the *Eoglobigerina trivialis* and *Subbotina triloculinoides* Subzones of the *P. pseudobulloides* Zone. The species ranges illustrated in Figure 1 are based on the stratigraphic distributions verified mainly in the El Kef stratotypic section. Note that the *Mh. holmdelensis* Subzone is equivalent to Zone P0 of Li and Keller (1998) and Berggren and Pearson (2005), whereas Zone Pα (or P1a of Li and Keller 1998) spans approximately the *Pv. longiapertura*, *Pv. sabina*, and *E. simplicissima* Subzones.

Arenillas et al. (2004) calibrated numerical ages of the biozonal boundaries on the basis of biostratigraphic and magnetostratigraphic data from Agost, Spain, and the timescale of Röhl et al. (2001), who astronomically calibrated the C29r/C29n reversal at 255 Kyr after the K/Pg boundary. Subsequent radiometric, paleomagnetic, and astronomical dating/calibrations have given different results for the age of the K/Pg boundary as well as the duration of the magnetozones. Taking into account the Geologic Time Scale 2012 (GTS12; Gradstein et al. 2012), which gives an age for the C29r/C29n boundary of 352 Kyr after the K/Pg boundary, the *Mh. holmdelensis* Subzone would span the first 7 Kyr after the K/Pg boundary, the *Pv. longiapertura* Subzone from 7 to 25 Kyr, the *Pv. sabina* Subzone from 25 to 46 Kyr, the *E. simplicissima* Subzone from 46 to 79 Kyr, the *E. trivialis* Subzone from 79 to 282 Kyr, and the *S. triloculinoides* Subzone from 282 to 616 Kyr.

High-resolution quantitative studies of Tethyan sections make it possible to recognize three planktic foraminiferal acme-stages (PFAS) of high biochronological interest across the lowermost Danian in pelagic (oceanic and outer neritic) environments (see Arenillas et al. 2006): PFAS-1, dominated by the triserial *Guembelitria*; PFAS-2, dominated by tiny trochospiral, informally denominated parvularugoglobigerinids (*Parvularugoglobigerina* and *Palaeoglobigerina*); and PFAS-3, dominated by biserial *Woodringina* and *Chiloguembelina*. Following the GTS12, PFAS-1 would span the first 18 Kyr after the K/Pg boundary, PFAS-2 approximately from 18 to 62 Kyr, and PFAS-3 from 62 Kyr on. A second acme of triserials is identified in the lower part of PFAS-3, that is, in the transition between the *Pv. eugubina* and *P. pseudobulloides* Zones (Arenillas et al.

https://doi.org/10.1017/pab.2018.16 Published online by Cambridge University Press

TABLE 1. Relative abundance (%) of planktic foraminiferal groups considered here and rates of aberrants at the El Kef section. Values for the hypotheses of both pattern A and pattern B are included. *A. m.*, *Abathomphalus mayaroensis* Zone; *P. h.*, *Plummerita hantkeninoides* Subzone; *H.* p., *Heterohelix* predominance; *P. e.*, *Parvularugoglobigerina eugubina* Zone; *P. s.*, *Palaeoglobigerina sabina* Subzone. Samples are presented in centimeters below (−) and above (+) the K/Pg boundary. x, relative abundance <0.3%.

El Kef														
Stage	Maastrichtian													
Zone	*Abathomphalus mayaroensis*													
Subzone	*Plummerita hantkeninoides*													
Acme-stage	*Heterohelix* predominance													
Sample	−1200	−1050	−900	−750	−540	−400	−250	−175	−135	−100	−70	−40	−20	−3
Total number of counted specimens	330	345	324	341	350	340	320	343	306	321	329	373	335	329
% Maastrichtian species	98.2	97.9	96.6	95.9	97.4	98.8	99.1	97.7	99.7	97.8	99.1	98.2	99.7	98.8
% triserial	1.8	2.1	3.4	4.1	2.6	1.2	0.9	2.3	0.3	2.2	0.9	1.8	0.3	1.2
Total number of aberrants	3	4	4	6	2	0	1	2	1	2	2	2	1	0
FAI (aberrant rate in %)	0.9	1.2	1.2	1.8	0.6		0.3	0.6	0.3	0.6	0.6	0.5	0.3	
% other Maastrichtian aberrants	0.9	1.2	1.2	1.5	0.6		0.3	0.6	0.3	0.6	0.6	0.5	0.3	
% triserial aberrants				0.3										

Hypothesis of pattern A												
Stage	Maastrichtian		Danian									
Zone	*A. m.*		*Guembelitria cretacea*								*P. e.*	
Subzone	*P. h.*		*Muricohedbergella holmdelensis*				*Parvularugoglobigerina longiapetura*				*P. s.*	
Acme-stage	*H.* p.	Barren interzone (airfall layer)	PFAS-1								PFAS-2	
Sample	0	+0.1	+2	+7	+17	+37	+67	+97	+122	+147	+172	+197
Total number of counted specimens	325		303	309	320	303	294	130	101	336	340	354
% other Maastrichtian species	98.8		83.1	83.0	45.1	10.3	2.7	7.4	3.9	4.8	0.9	0.6
% triserial	1.2		16.9	17.0	54.9	89.7	87.0	66.7	80.3	69.8	27.0	7.8
% parvularugoglobigerinids						x	9.5	21.8	15.6	26.4	71.0	91.9
% Danian biserial							0.7	2.2	x	0.3	0.9	x
Total number of aberrants	1		1	7	25	41	55	23	9	27	37	38
FAI (aberrant rate in %)	0.3		0.3	2.3	7.8	13.5	18.7	17.7	8.9	8.0	10.9	10.7
% other Maastrichtian aberrants	0.3			0.3								
% triserial aberrants			0.3	1.9	7.8	13.5	17.7	9.2	6.9	4.8	3.5	0.8
% parvularugoglobigerinid aberrants							1.0	8.5	2.0	3.3	7.4	9.9

Stage	Danian													
Zone	*Parvularugoglobigerina eugubina*						*Parasubbotina pseudobulloides*							
Subzone	*P. s.*	*Eoglobigerina simplicissima*					*Eoglobigerina trivialis*				*Subbotina triloculinoides*			
Acme-stage	PFAS-2						PFAS-3							
Sample	+247	+297	+372	+447	+547	+647	+747	+847	+922	+992	+1107	+1197	+1277	+1347
Total number of counted specimens	356	358	381	409	360	677	473	366	460	398	369	408	405	470
% other Maastrichtian species	x	0.8	0.6	1.7	0.3	1.1	1.0	1.1	3.5	1.1	0.6	0.6		
% triserial	8.6	4.5	2.9	3.5	1.2	31.1	59.9	54.3	28.3	18.5	7.0	3.6	4.6	7.4
% parvularugoglobigerinids	90.3	70.1	70.1	53.5	11.6	7.7	0.2	0.5	0.4					
% Danian biserial	1.4	23.7	17.0	28.3	77.6	53.9	36.1	41.1	53.8	56.9	59.5	59.3	62.2	55.3
% other Danian species		0.8	8.6	8.9	9.1	5.4	2.2	2.9	12.7	22.6	31.1	36.2	35.4	27.9
Total number of aberrants	26	11	27	33	30	67	52	32	22	19	14	13	10	17
FAI (aberrant rate in %)	7.3	3.1	7.1	8.1	8.3	9.9	11.0	8.7	4.8	4.8	3.8	3.2	2.5	3.6
% triserial aberrants	0.8	0.3	0.3	1.2	0.3	4.1	6.6	5.0	1.4	1.0	0.3	0.5		
% parvularugoglobigerinid aberrants	7.0	1.7	6.0	4.2	0.8	1.6	0.2	0.3						
% Danian biserial aberrants		0.6	0.8	2.0	6.4	3.8	4.2	3.6	2.8	2.5	3.0	1.5	2.0	2.3
% other Danian aberrants				0.7	0.8	0.3			0.7	1.3	0.5	1.2	0.5	1.3

Hypothesis of pattern B

Stage	Maastrichtian		Danian									
Zone	*A. m.*		*Guembelitria cretacea*								*P. e.*	
Subzone	*P. h.*		*Muricohedbergella holmdelensis*				*Parvularugoglobigerina longiapetura*				*P. s.*	
Acme-stage	*H.* p.	Barren interzone (airfall layer)	PFAS-1								PFAS-2	
Sample	0	+0.1	+2	+7	+17	+37	+67	+97	+122	+147	+172	+197
Total number of counted specimens	325		51	53	176	272	285	118	97	325	337	354
% other Maastrichtian species	98.8											
% triserial	1.2		100.0	100.0	100.0	100.0	89.8	73.7	83.5	72.3	27.3	7.9
% parvularugoglobigerinids						x	9.5	23.7	16.5	27.4	71.8	92.1
% Danian biserial							0.7	2.5	x	0.3	0.9	x
Total number of aberrants	1		1	6	25	41	55	23	9	27	37	38
FAI (aberrant rate in %)	0.3		2.0	13.2	14.2	15.1	19.3	19.5	9.3	8.3	11.0	10.7
% other Maastrichtian aberrants	0.3											
% triserial aberrants			2.0	13.2	14.2	15.1	18.2	10.2	7.2	4.9	3.6	0.8
% parvularugoglobigerinid aberrants							1.1	9.3	2.1	3.4	7.4	9.9

TABLE 1. *CONTINUED*

Stage	Danian													
Zone	*Parvularugoglobigerina eugubina*						*Parasubbotina pseudobulloides*							
Subzone	*P. s.*	*Eoglobigerina simplicissima*					*Eoglobigerina trivialis*				*Subbotina triloculinoides*			
Acme-stage	PFAS-2				PFAS-3									
Sample	+247	+297	+372	+447	+547	+647	+747	+847	+922	+992	+1107	+1197	+1277	+1347
Total number of counted specimens	356	358	381	409	360	677	473	366	460	398	369	408	405	470
% other Maastrichtian species	x	0.8	0.6	1.7	0.3	1.1	1.0	1.1	3.5	1.1	0.6	0.6		
% triserial	8.6	4.5	2.9	3.5	1.2	31.1	59.9	54.3	28.3	18.5	7.0	3.6	4.6	7.4
% parvularugoglobigerinids	90.3	70.1	70.1	53.5	11.6	7.7	0.2	0.5	0.4					
% Danian biserial	1.4	23.7	17.0	28.3	77.6	53.9	36.1	41.1	53.8	56.9	59.5	59.3	62.2	55.3
% other Danian species		0.8	8.6	8.9	9.1	5.4	2.2	2.9	12.7	22.6	31.1	36.2	35.4	27.9
Total number of aberrants	26	11	27	33	30	67	52	32	22	19	14	13	10	17
FAI (aberrant rate in %)	7.3	3.1	7.2	8.1	8.4	10.1	11.1	8.8	5.0	4.8	3.9	3.2	2.5	3.6
% triserial aberrants	0.3	0.8	0.3	1.2	0.3	4.2	6.6	5.0	1.4	1.0	0.3	0.5		
% parvularugoglobigerinid aberrants	7.0	1.7	6.1	4.2	0.8	1.6	0.2	0.3						
% Danian biserial aberrants		0.6	0.8	2.0	6.4	3.9	4.3	3.6	2.9	2.5	3.0	1.5	2.0	2.3
% other Danian aberrants				0.7	0.8	0.3			0.7	1.3	0.6	1.2	0.5	1.3

TABLE 2. Relative abundance (%) of planktic foraminiferal groups considered here and rates of aberrants at the Aïn Settara section. Values for the hypotheses of both pattern A and pattern B are included. *A. m.*, *Abathomphalus mayaroensis* Zone; *P. h.*, *Plummerita hantkeninoides* Subzone; *H.* p., *Heterohelix* predominance. Samples are stated in centimeters below (–) and above (+) the K/Pg boundary.

Aïn Settara													
Stage	Maastrichtian												
Zone	*Abathomphalus mayaroensis*												
Subzone	*Plummerita hantkeninoides*												
Acme-stage	*Heterohelix* predominance												
Sample	–640	–540	–340	–240	–140	–90	–40	–31	–21	–13	–11	–6	–2
Total number of counted specimens	333	319	319	293	294	330	302	310	340	334	307	304	318
% Maastrichtian species	93.1	94.0	97.5	99.0	98.3	97.3	98.7	98.0	98.2	98.2	95.8	99.1	96.6
% triserial	6.9	6.0	2.5	1.0	1.7	2.7	1.3	2.0	1.8	1.8	4.2	0.9	3.4
Total number of aberrants	12	11	5	3	2	6	3	6	7	6	7	5	3
FAI (aberrant rate in %)	3.6	3.4	1.6	1.0	0.7	1.8	1.0	1.9	2.1	1.8	2.3	1.6	0.9
% other Maastrichtian aberrants	3.0	2.8	1.6	1.0	0.7	1.8	1.0	1.9	2.1	1.8	2.3	1.6	0.9
% triserial aberrants													

Hypothesis of pattern A											
Stage	Maastrichtian		Danian								
Zone	*A. m.*		*Guembelitria cretacea*								
Subzone	*P. h.*		*Muricohed. holmdelensis*			*Parvularugoglobigerina longiapetura*					
Acme-stage	*H.* p.	Barren interzone (airfall layer)	PFAS-1				PFAS-2				
Sample	–1	+4-5	+5	+10	+15	+20	+30	+40	+45	+50	+55
Total number of counted specimens	315		293	293	264	298	257	307	334	334	342
% other Maastrichtian species	95.3		86.8	71.4	25.0	29.0	22.0	7.0	6.8	2.7	3.6
% triserial	4.7		12.2	24.7	68.8	60.4	33.1	29.0	34.7	28.7	23.4
% parvularugoglobigerinids					4.1	10.3	44.9	63.4	58.4	68.5	72.6
Total number of aberrants	6		10	17	33	33	20	17	23	16	18
FAI (aberrant rate in %)	1.9		3.4	5.8	12.1	10.7	8.2	5.5	7.2	4.8	5.6
% other Maastrichtian aberrants	1.9		1.0	1.4	1.9	0.7	0.4				
% triserial aberrants			2.4	5.8	9.8	8.1	3.5	1.0	1.5	1.2	0.3
% parvularugoglobigerinid aberrants					1.5	3.0	4.3	4.6	5.7	3.6	5.3

TABLE 2. *CONTINUED*

Stage	Danian											
Zone	*Parvularugoglobigerina eugubina*								*Parasubbotina pseudobulloides*			
Subzone	*Parvularugoglobigerina sabina*				*Eoglobigerina simplicissima*				*Eoglobigerina trivialis*			
Acme-stage	PFAS-2							PFAS-3				
Sample	+60	+80	+110	+130	+160	+260	+360	+460	+560	+660	+860	+1040
Total number of counted specimens	246	273	295	271	272	310	317	262	331	387	307	304
% other Maastrichtian species	8.4	6.2	10.5	2.9	5.6	5.3	4.0	16.3	4.5	7.6	1.6	
% triserial	24.3	6.9	12.8	12.9	9.1	3.2	4.3	30.0	36.6	15.5	14.6	2.0
% parvularugoglobigerinids	66.1	86.7	77.3	82.5	66.3	71.2	72.3	4.2	2.4	4.9		
% Danian biserial				0.4	14.2	18.7	16.4	39.6	46.0	59.8	49.8	39.7
% other Danian species							1.8	10.1	10.4	13.3	30.6	48.4
Total number of aberrants	22	19	19	20	16	17	18	24	34	6	6	5
FAI (aberrant rate in %)	8.1	7.0	6.4	7.4	5.9	5.5	5.7	9.2	10.3	1.6	2.0	1.6
% triserial aberrants	2.4	0.7	0.7	1.1	0.7			5.7	3.0	0.5		
% parvularugoglobigerinid aberrants	5.7	6.2	5.8	6.3	3.7	2.9	4.4					
% Danian biserial aberrants					1.5	2.6	1.3	3.4	4.8	0.5	1.6	0.7
% other Danian aberrants									0.3	0.5	0.3	1.0

Hypothesis of pattern B

Stage	Maastrichtian		Danian								
Zone	*A. m.*		*Guembelitria cretacea*								
Subzone	*P. h.*		*Muricohed. holmdelensis*			*Parvularugoglobigerina longiapetura*					
Acme-stage	*H.* p.	Barren interzone (airfall layer)	PFAS-1			PFAS-2					
Sample	−1	+4-5	+5	+10	+15	+20	+30	+40	+45	+50	+55
Total number of counted specimens	315		39	81	198	212	200	285	311	325	330
% other Maastrichtian species	95.3										
% triserial	4.7		100.0	100.0	94.4	85.4	42.4	31.4	37.3	29.5	24.4
% parvularugoglobigerinids					5.6	14.6	57.6	68.6	627.0	70.5	75.6
Total number of aberrants	6		7	13	31	35	20	17	23	16	18
FAI (aberrant rate in %)	1.9		17.9	16.0	15.2	14.2	10.0	6.0	7.7	4.9	5.8
% other Maastrichtian aberrants	1.9										

% triserial aberrants	17.9	16.0	13.1	11.3	4.5	1.1	1.6	1.2	0.3	
% parvularugoglobigerinid aberrants			2.5	4.2	5.5	4.9	6.1	3.7	5.5	
% Danian biserial aberrants										
% other Danian aberrants										

Stage	Danian										
Zone	*Parvularugoglobigerina eugubina*							*Parasubbotina pseudobulloides*			
Subzone	*Parvularugoglobigerina sabina*				*Eoglobigerina simplicissima*			*Eoglobigerina trivialis*			
Acme-stage	PFAS-2							PFAS-3			
Sample	+60	+80	+110	+130	+160	+260	+360	+460	+560	+660	+860	+1040
Total number of counted specimens	225	256	264	263	257	294	304	219	316	358	302	304
% other Maastrichtian species												
% triserial	26.9	7.4	14.2	13.5	10.2	3.4	4.5	35.8	38.4	16.6	15.4	2.2
% parvularugoglobigerinids	73.1	92.6	85.8	86.1	74.0	76.5	76.3	5.0	2.5	5.2		
% Danian biserial				0.4	15.8	20.1	17.3	47.2	48.2	64.0	52.4	44.1
% other Danian species							1.9	12.0	10.9	14.2	32.2	53.7
Total number of aberrants	22	19	19	20	16	17	18	24	34	6	6	5
FAI (aberrant rate in %)	8.9	7.4	7.2	8.7	6.2	5.8	5.9	11.0	10.8	1.7	2.0	1.6
% triserial aberrants	2.7	0.8	0.8	1.1	0.8			5.7	4.7	0.6		
% parvularugoglobigerinid aberrants	6.2	6.6	6.4	6.5	3.9	3.1	4.6					
% Danian biserial aberrants					1.6	2.7	1.3	3.4	5.7	0.6	1.7	0.7
% other Danian aberrants									0.3	0.6	0.3	1.0

2017). This acme has been attributed to the genus *Chiloguembelitria* Hofker, 1978, not *Guembelitria*, and spans approximately from 70 to 200 Kyr according to the GTS12.

Danian Planktic Foraminiferal Evolutionary Radiations

Many new species of trochospiral and biserial planktic foraminifers originated after the K/Pg boundary, as is shown in Figure 1 and described in Supplementary Appendix A. The systematic scheme in Supplementary Figure 1 is a good reflection of the morphological and textural diversity that appeared after the extinction event. As illustrated in Figure 1, the planktic foraminifera evolutionary radiation of the early Danian happened in two pulses (see also Arenillas et al. 2000a,b, 2017; Arenillas and Arz 2017). The first occurred between approximately 5 and 26 Kyr after the K/Pg boundary according to the GTS12, with the appearance of tiny, trochospiral species belonging to the parvularugoglobigerinids (*Pseudocaucasina*, *Palaeoglobigerina*, and *Parvularugoglobigerina*) and biserial taxa (*Woodringina* and *Chiloguembelina*), as well as triserial species of the genus *Chiloguembelitria* (Supplementary Figs. 1 and 2). The second evolutionary radiation occurred between approximately 46 and 110 Kyr after the K/Pg boundary according to the GTS12, giving rise to more ornamented, larger trochospiral species (Supplementary Figs. 1, 3) belonging to *Trochoguembelitria*, *Eoglobigerina*, *Parasubbotina*, *Globanomalina*, and *Praemurica*. Other genera appear shortly afterward, such as *Subbotina* and *Globoconusa*.

In the present work, the extinction and evolution of planktic foraminifers across the K/Pg boundary at the El Kef section were quantified using the evolutionary model proposed by Dean and McKinney (2001), which measures taxonomic turnovers using four metrics (Fig. 2): extinction rate (E_R), speciation rate (N_R), volatility (V), and taxonomic flux (F). Taxonomic flux F is used to estimate whether there are relative increases (positive values) or declines (negative values) in diversity. The volatility V indicates whether there is evolutionary stability (low values) or increased taxonomic turnover (high values). The method developed by Dean and McKinney (2001), which is described in Supplementary Appendix B, was applied to the stratigraphic ranges of planktic foraminiferal species recognized in the El Kef section (Supplementary Fig. 4). The present quantification of the evolutionary pattern is an update of the one already made at El Kef by Arenillas et al. (2002), taking into account the taxonomic and biostratigraphic revisions made since then (see Supplementary Appendix A). The metrics were measured under two alternative hypotheses, as already proposed by Arenillas et al. (2002): (1) all 16 Cretaceous species identified in lower Danian levels are in situ (pattern A in Supplementary Table 1): *Muricohedbergella holmdelensis*, *Muricohedbergella monmouthensis*, *Heterohelix globulosa*, *Heterohelix planata*, *Heterohelix navarroensis*, *Heterohelix labellosa*, *Laeviheterohelix pulchra*, *Laeviheterohelix glabrans*, *Pseudoguembelina kempensis*, *Pseudoguembelina costulata*, *Globigerinelloides volutus*, *Globigerinelloides praeriehillensis*, *Globigerinelloides yaucoensis*, *Guembelitria dammula*, *Guembelitria cretacea*, and *Guembelitria blowi* (see Supplementary Fig. 4); and (2) except for two *Guembelitria* species (*Guembelitria cretacea* and *Guembelitria blowi*), all Cretaceous species identified in lower Danian levels are reworked (pattern B in Supplementary Table 2).

According to these metrics, in both hypotheses (Fig. 2), four main evolutionary episodes were recognized: (1) an extremely high extinction rate coinciding with the catastrophic mass extinction at the K/Pg boundary; (2) a high speciation rate in the *Pv. longiapertura* Subzone coinciding with the first Danian evolutionary radiation, mainly of parvularugoglobigerinids; (3) a relatively high speciation rate in the *E. simplicissima* Subzone coinciding with the beginning of the second evolutionary radiation; and (4) a relatively high extinction rate in the basal part of the *E. trivialis* Subzone coinciding with the parvularugoglobigerinid extinction. Due to these evolutionary episodes, volatility is high at El Kef during approximately the first 200 Kyr of the Danian, which is also reflected by relevant fluctuations in the taxonomic flux. These data contrast with the extremely low volatility in the *P. hantkeninoides* Subzone of the uppermost Maastrichtian (Fig. 2).

https://doi.org/10.1017/pab.2018.16 Published online by Cambridge University Press

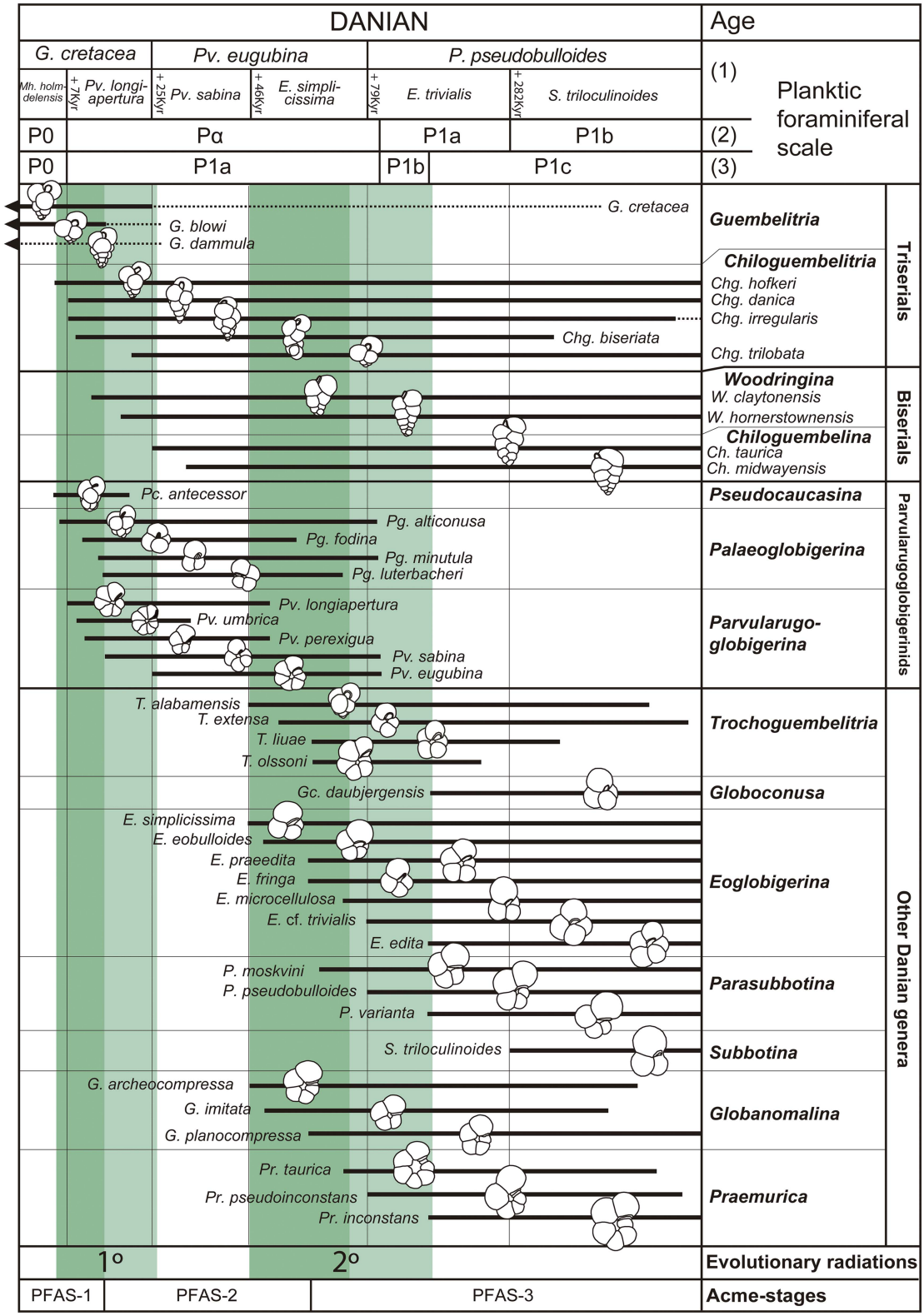

https://doi.org/10.1017/pab.2018.16 Published online by Cambridge University Press

Abnormal Specimens across the K/Pg Boundary

Our quantitative study of planktic foraminifers has revealed a strong proliferation of aberrant forms above the K/Pg boundary in the El Kef and Aïn Settara sections (Fig. 3). At El Kef, the abundance of aberrant tests (Foraminiferal Abnormality Index, or FAI) in PFAS-1 is as high as 18.7% of the total population of planktic foraminifera, of which almost 90% are abnormal forms of the triserial *Guembelitria*. At Aïn Settara, the abundance of aberrant forms in PFAS-1 reaches over 12%, of which almost 70% are aberrant tests belonging to *Guembelitria*. These data contrast with the total percentage of aberrant tests in studied Maastrichtian samples (Tables 1, 2), which almost never exceeds 2.5% in either section (except for the basal part of the Aïn Settara section, whose FAI is as high as 3.4–3.6%). These include a few aberrant specimens, mainly of *Heterohelix* and *Pseudoguembelina.*

These percentages increase if we assume that the Maastrichtian specimens found in Danian horizons are reworked (pattern B hypothesis), except for two *Guembelitria* species (curves with black shading in Fig. 3). In this case, the FAI in PFAS-1 reaches almost 20% in El Kef and 18% in Aïn Settara. It should be noted that, except for *Guembelitria*, the percentages of other aberrant Maastrichtian specimens in the Danian are similar to those estimated for Maastrichtian horizons (Tables 1, 2), in contrast with the strong increase in aberrant tests among the Danian *Guembelitria* specimens within the dark-clay bed. This suggests that all these Maastrichtian specimens (aberrants and non-aberrants alike) are in fact reworked. A high-resolution biostratigraphic analysis at the Moncada section, Cuba, revealed that, with the exception of *Guembelitria* species, there were no cosmopolitan, generalist Cretaceous species in the lowermost Danian deposits, not even in Zone P0 and the dark-clay bed (Arenillas et al. 2016). This evidence led the authors to suggest that the planktic foraminiferal mass extinction at the K/Pg boundary was more severe and catastrophic than previously suggested and that the presence of Cretaceous species within the lowermost Danian deposits at most K/Pg localities may be the result of normal reworking/bioturbation processes worldwide (see also Huber 1996; Kaiho and Lamolda 1999; Huber et al. 2002). In any case, whether we consider the pattern A hypothesis or that of pattern B, the abundance curves indicate similar trends (Fig. 3).

Aberrant *Guembelitria* specimens have frequently been classified as *Guembelitria irregularis* (e.g., Coccioni and Luciani 2006). This species has no doubt been used as a "wastebasket" taxon that also includes the aberrant forms of both Maastrichtian and Danian guembelitriids (see discussion in Arz et al. 2010). However, we consider here that *irregularis* is a genuine Danian species, including normal triserial forms (see Supplementary Fig. 1), because the abnormal morphologies among guembelitriids are of another kind. Arenillas et al. (2017) attributed *irregularis* to the genus *Chiloguembelitria* instead of *Guembelitria*, on the basis of differences in the wall texture and position of the aperture. *Chiloguembelitria irregularis* groups Danian specimens with twisted triserial arrangements of irregular appearance, corresponding to the irregular morphophase of the model of Tyszka (2006). Nevertheless, if these specimens are also counted as abnormal forms, then the FAI during the earliest Danian is even more anomalous, reaching more than 23% in PFAS-1 at El Kef, according to the pattern B hypothesis (Fig. 3).

FIGURE 1. Biostratigraphic ranges of the early Danian species analyzed, based mainly on the El Kef and Aïn Settara sections, Tunisia; (1) planktic foraminiferal zonation and calibrated numerical ages of the biozonal boundaries proposed by Arenillas et al. (2004); (2) and (3) zonations of Berggren and Pearson (2005) and Li and Keller (1998), respectively; intervals with green shading indicate the first and second evolutionary radiations of the early Danian at El Kef (the shading in dark green indicates high speciation rates; see online version for color); dotted lines indicate uncertain ranges in the case of *Guembelitria* species (*G. cretacea*, *G. blowi*, and *G. dammula*) in the lower Danian, because these may actually correspond to reworked specimens and/or the ranges of morphologically similar species of *Chiloguembelitria* (*Chg. danica*, *Chg. trilobata*, and *Chg. hofkeri*, respectively). PFAS, planktic foraminiferal acme-stage.

https://doi.org/10.1017/pab.2018.16 Published online by Cambridge University Press

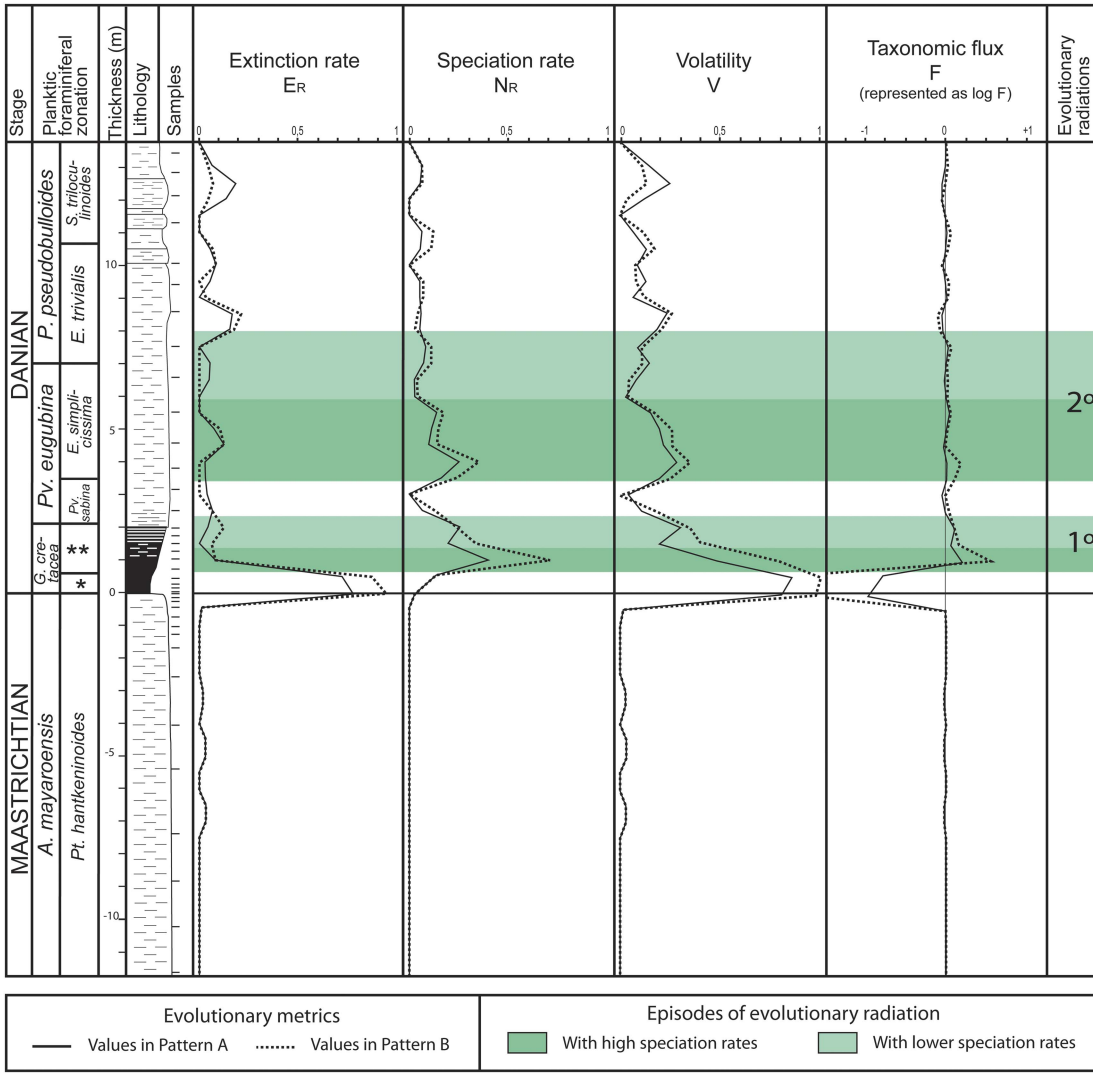

FIGURE 2. Evolutionary metrics (extinction and speciation rates, volatility, and taxonomic flux) at El Kef according to the model of Dean and McKinney (2001); solid line, hypothesis of pattern A; dotted line, hypothesis of pattern B; green shading, episodes of evolutionary radiation, with shading in dark green to indicate high speciation rates (see online version for color). **Mh. holmdelensis* Subzone (= Zone P0); ***Pv. longiapertura* Subzone.

During the episode PFAS-1, abnormalities are frequent in all planktic foraminiferal groups, suggesting that ecological stress affected all pelagic environments during the early Danian. The FAI in the upper PFAS-1 is high not only in guembelitriids but also in parvularugoglobigerinids; for example, almost 40% of parvularugoglobigerinid specimens from the sample at 97 cm above the K/Pg boundary at El Kef have some type of abnormality. Subsequently, the abundance of aberrant tests decreases during PFAS-2 but remains relatively high in both El Kef and Aïn Settara, at around 3–10% (in both patterns A and B), suggesting that the environmental conditions remained unstable tens of thousands of years after the K/Pg boundary. Another increase in the FAI has been recognized across the boundary between the *Pv. eugubina* and *P. pseudobulloides* Zones (mainly in the *E. trivialis* Subzone, or Subzone P1a), rising to a maximum of 11% (in both patterns A and B) in El Kef and Aïn Settara (Fig. 3). The increase in aberrant forms is more evident

https://doi.org/10.1017/pab.2018.16 Published online by Cambridge University Press

among triserial and biserial specimens of the genera *Chiloguembelitria*, *Woodringina*, and *Chiloguembelina*. This interval coincides with the second bloom of triserials in the lower part of PFAS-3 (Fig. 3), in this case caused by *Chiloguembelitria* and not by *Guembelitria*. *Guembelitria* comprised opportunistic species whose relative abundance strongly increased in ecological stress conditions, mainly related to eutrophication episodes (see e.g., Keller and Pardo 2004). *Chiloguembelitria* replaced *Guembelitria* in the early Danian, occupying a similar ecological niche (Arenillas et al. 2017), so its blooms indicate similar conditions of ecological stress. Maxima in aberrant specimens thus seem to coincide with guembelitriid blooms in the early Danian, as occurs in PFAS-1 and the lower part of PFAS-3.

A Compendium of Earliest Danian Abnormal Morphologies

Various types of abnormalities are present among the earliest Danian planktic foraminifers, severely complicating their taxonomic identification in some cases. Abnormal specimens have previously been reported in the lowermost Danian of other localities, mainly among *Guembelitria* (Coccioni and Luciani 2006) but also among parvularugoglobigerinids (Gerstel et al. 1986). Double and multiple tests of *Parasubbotina* and *Globoconusa* were also described by Ballent and Carignano (2008) in shallow environments of the Cerro Azul section, Argentina.

The terminology used here to describe the abnormalities identified in the earliest Danian (Figs. 4, 5) is based on those of Polovodova and Schönfeld (2008), Ballent and Carignano (2008), and Montgomery (1990) for both benthic and planktic foraminifera. The specimens illustrated in Figures 6 and 7 and Supplementary Figures 5, 6, and 7 come mainly from El Kef and Aïn Settara, but also from Elles, Agost, and Caravaca. The aberrant morphologies identified belong to the following categories:

1. Protuberance near the proloculus, which includes two types: (a) protruding proloculus (Fig. 4A1); and (b) second chamber abnormally protruding beside the proloculus (Fig. 4A2), also known as a double- or twinned-chamber arrangement. The latter occurs during the calcification of juvenile individuals and may be a result of frustrated double tests (Stouff et al. 1999). During the early ontogenetic stage, two chambers can grow from the proloculus with subsequent development of an independent whorl from each of the second chambers; if a single whorl develops from one of these chambers, then the other appears as a protuberance on the proloculus (Polovodova and Schönfeld 2008).

2. Chamber abnormalities, which include six types: (a) aberrant shapes (Fig. 4B1); (b) reduced chamber sizes (Fig. 4B2); (c) overdeveloped chambers of the last whorl (Fig. 4B3); (d) additional chambers (Fig. 4B4); (e) protuberant chambers (Fig. 4B5); and (d) welded chambers (Fig. 4B6). Overdeveloped and reduced chambers have been related to environmental stress (Hecht and Savin 1972). For benthic foraminifera, Sujata et al. (2011) proposed that abnormal chambers are a result of specimens being subjected to temporary hyposaline conditions, which causes considerable dissolution and the subsequent regeneration of the chamber in an abnormal form. The same phenomenon could be applied to planktic foraminifera in conditions of acidified waters with increased carbonate dissolution, as occur in global warming–hyperthermal episodes (e.g., Luciani et al. 2007).

3. Abnormal ultimate chamber, which includes five types: (a) aberrant shape (Fig. 4C1); (b) kummerform, or reduced last chamber (Fig. 4C2); (c) overdeveloped or inflated last chamber (Fig. 4C3); (d) anomalous position (Fig. 4C4) causing, for example, the change from biserial/triserial to uniserial; and (e) bulla-like chamber (Fig. 4C5), that is, the last chamber partially or totally covering the umbilicus, resembling a bulla. The first three types are identified here in all the planktic foraminiferal groups and are frequently associated with a decrease in ornamentation. The bulla-like last chamber is typical of high trochospiral specimens with an intraumbilical or quasi-intraumbilical aperture, as in some species of *Palaeoglobigerina* and *Parvularugoglobigerina*.

https://doi.org/10.1017/pab.2018.16 Published online by Cambridge University Press

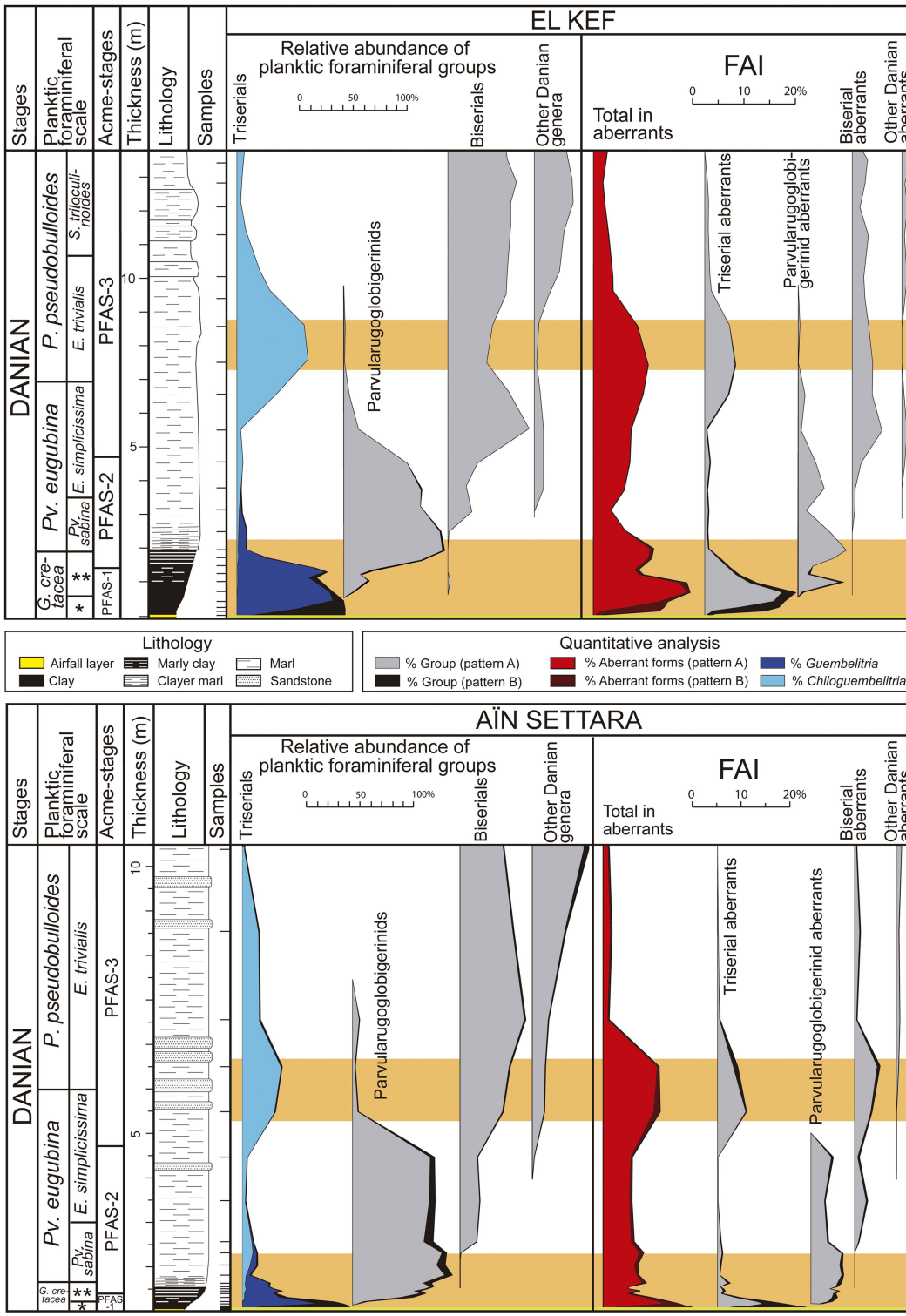

FIGURE 3. Quantitative stratigraphic distribution of planktic foraminiferal groups and aberrant forms across the K/Pg boundary in the El Kef and Aïn Settara sections. The triserial group includes *Guembelitria* and *Chiloguembelitria*; the parvularugoglobigerinids include *Pseudocaucasina*, *Palaeoglobigerina*, and *Parvularugoglobigerina*; the biserial group

https://doi.org/10.1017/pab.2018.16 Published online by Cambridge University Press

Hecht and Savin (1972) reported that bulla-like abnormal chambers are more common in warmer waters and seem to develop on unusually long-lived specimens (Montgomery 1990). According to Bijma et al. (1992), abnormal last chambers could be induced by the ocean oxygen level, light quality, or feeding rate. Saclike overdeveloped chambers seem currently to be more common in upwelling areas characterized by waters that are more anoxic and richer in nutrients and in more yellow-green light conditions. Kummerform chambers are probably the result of the opposite conditions, that is, more oxygenated waters, oligotrophy, and light conditions (blue) typical of the open ocean.

4. Multiple ultimate chambers, which include two types: (a) double or twinned ultimate chambers (Fig. 4D1); and (b) proliferation of chambers in the last whorl(s) (Fig. 4D2). They are present mostly in triserial species (*Guembelitria*), but are also found here in the trochospiral *Palaeoglobigerina*. In *Guembelitria*, these additional chambers are usually disposed in several directions (multiserial forms). Many triserial specimens exhibit an ultimate tetraserial stage and have probably been misidentified as *Palaeoglobigerina alticonusa* and/or *Trochoguembelitria alabamensis* (see Supplementary Fig. 1). Others, mainly biserials, have two complete and identical ultimate chambers. According to Venturati (2006), twinned or bilobated chambers may be used as potential proxies for environmental stress. Montgomery (1990) suggested that specimens with multiple last chambers could also be some type of gerontic kummerforms, because these chambers tend to be downsized and similar in shape, and this could indicate long life.

5. Abnormal apertures, which include three types: (a) aberrant shape (e.g., gaping aperture), usually associated with abnormal ultimate chambers (Fig. 5E1); (b) additional aperture (Fig. 5E2); and (c) multiple apertures (Fig. 5E3), usually associated with multiple ultimate chambers. According to Montgomery (1990), gaping apertures represent a strategy directly opposed to that of apertures covered by bullae, whose function is to protect them.

6. Distortion in test coiling, which includes three types: (a) excessively high spiral side or spiroconvex test (Fig. 5F1); (b) kinking (Fig. 5F2), that is, abnormal coiling due to a change in the direction of coiling, with two or more axes of rotation; and (c) twisting of entire test or extreme kinking (Fig. 5F3), that is, the umbilical side becomes the spiral side. Distortion in test coiling also seems to be a response to very stressed environments (Montogomery 1990; Polovodova and Schönfeld 2008).

7. Abnormal test, which includes four types: (a) lack of sculpture (Fig. 5G1); (b) poor development of the last whorl (Fig. 5G2); (c) overdevelopment of the last whorl (Fig. 5G3); and (d) compressed test (Fig. 5G4). Another test abnormality is a lack of ornamentation, but this type is not been analyzed here due to the difficulty of demonstrating the difference between abnormal alterations in the wall surface and the diagenetic processes of dissolution/recrystallization, which are usual in El Kef and Aïn Settara. As in the previous category, these abnormalities also seem to be a response to stressed environments (Polovodova and Schönfeld 2008), in some cases due to extremely stressful shifts in the environment (Montgomery 1990).

8. Attached twins or double tests, which include two types: (a) attached twins (Siamese) (Fig. 5H1), or even attached triplets (triamese) (Fig. 6.C); and (b) fused test (Fig. 5H2). If a second chamber beside the proloculus is followed by the development of an adjacent whorl, with two whorls with a similar number of chambers developing synchronously, attached twins are formed. Stouff et al. (1999) proposed

←
includes *Woodringina* and *Chiloguembelina*; and other Danian genera include *Trochoguembelitria*, *Eoglobigerina*, *Parasubbotina*, *Globanomalina*, *Praemurica*, *Subbotina*, and *Globoconusa*. Curves with black shading represent the recalculated percentages assuming that, except for *Guembelitria*, the Maastrichtian specimens found in Danian horizons are reworked (pattern B hypothesis). Intervals with orange shading (see online version for color) represent terminal stress levels according to the model of Weinkauf et al. (2014). FAI, Foraminiferal Abnormality Index (% aberrant planktic foraminifera). **Mh. holmdelensis* Subzone (= Zone P0); ***Pv. longiapertura* Subzone.

https://doi.org/10.1017/pab.2018.16 Published online by Cambridge University Press

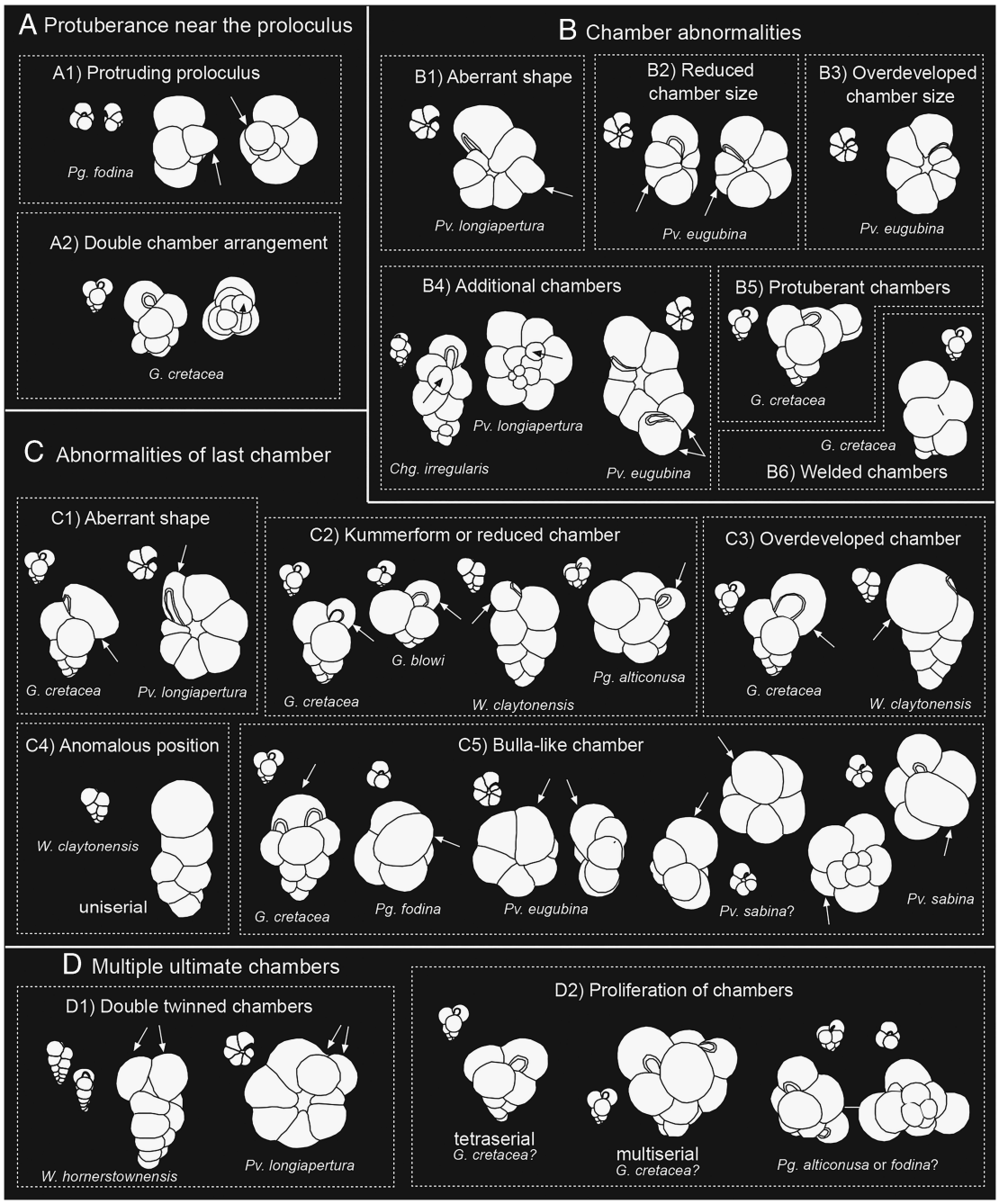

FIGURE 4. Schematic diagram of the main types of aberrant forms in the following categories: A, protuberances near the proloculus; B, chamber abnormalities; C, abnormalities of last chamber, including kummerforms; and D, multiple ultimate chambers, including double or twinned ultimate chambers (see explanation in text). Correlative normal forms are represented in miniature along with the abnormal forms.

that double tests in benthic foraminifera may result from: (i) an anomaly in the development of a single juvenile, building two or three second chambers or two third chambers, each one possibly developing in an individual whorl; (ii) the early fusion of two juveniles, which both develop after their fusion; (iii) the attachment of a juvenile to a parental test after schizogony,

https://doi.org/10.1017/pab.2018.16 Published online by Cambridge University Press

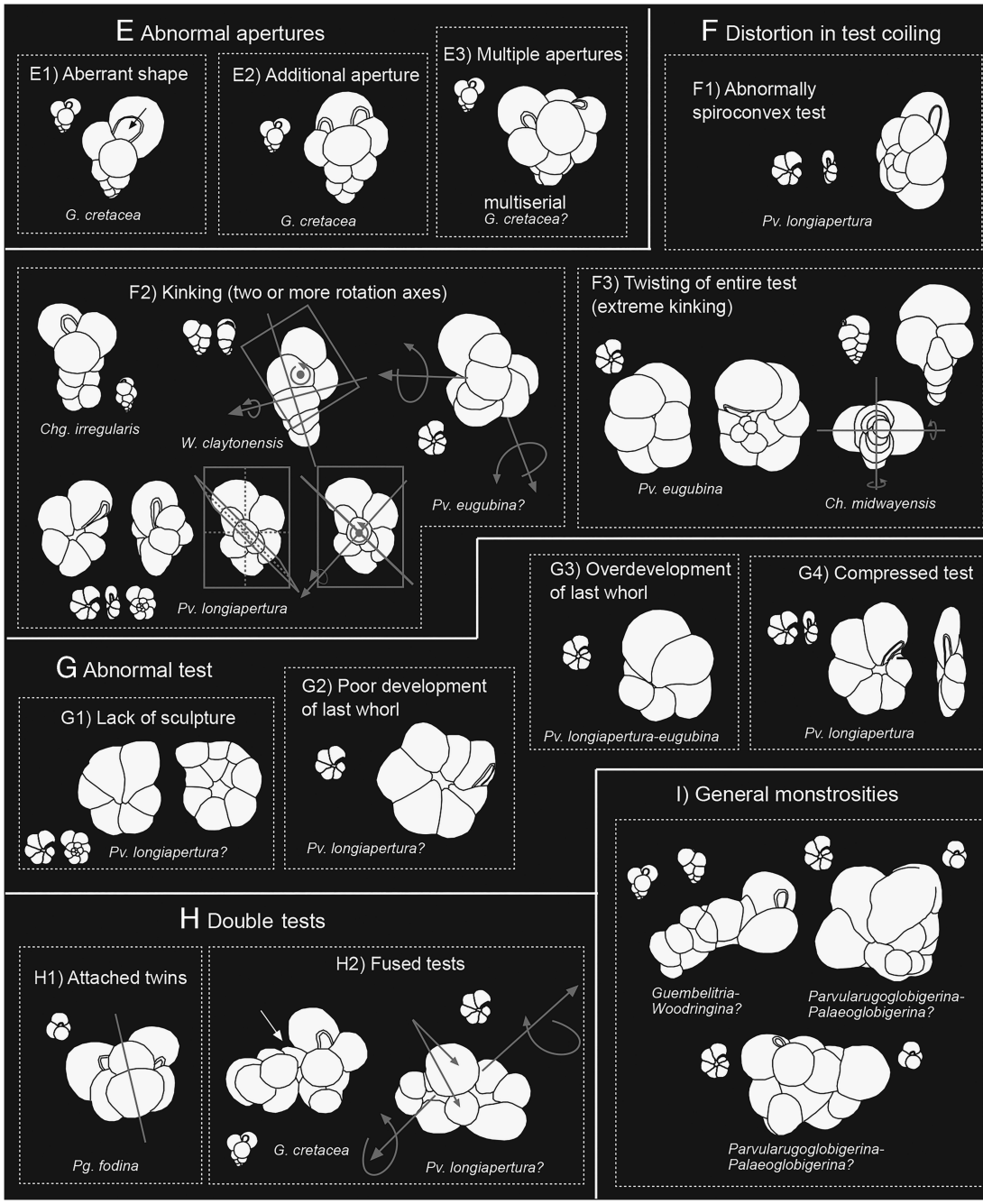

FIGURE 5. Schematic diagram of the main types of aberrant forms in the following categories (continuing from Fig. 4): E, abnormal apertures, including multiple apertures; F, distortion in test coiling, including kinking; G, morphologically abnormal tests; H, double tests, including attached twins or fused tests; and I, general monstrosities (see explanation in text). Correlative normal forms are represented in miniature along with the abnormal forms.

followed by the development of the juvenile specimen. According to Montgomery (1990), twinned specimens indicate reproductive difficulties in stressed environments.

9. General monstrosities (Fig. 5I): a conjunction of abnormal coiling due to several wrong directions of coiling, bulla-like kummerform chambers, double tests, and multiple ultimate

https://doi.org/10.1017/pab.2018.16 Published online by Cambridge University Press

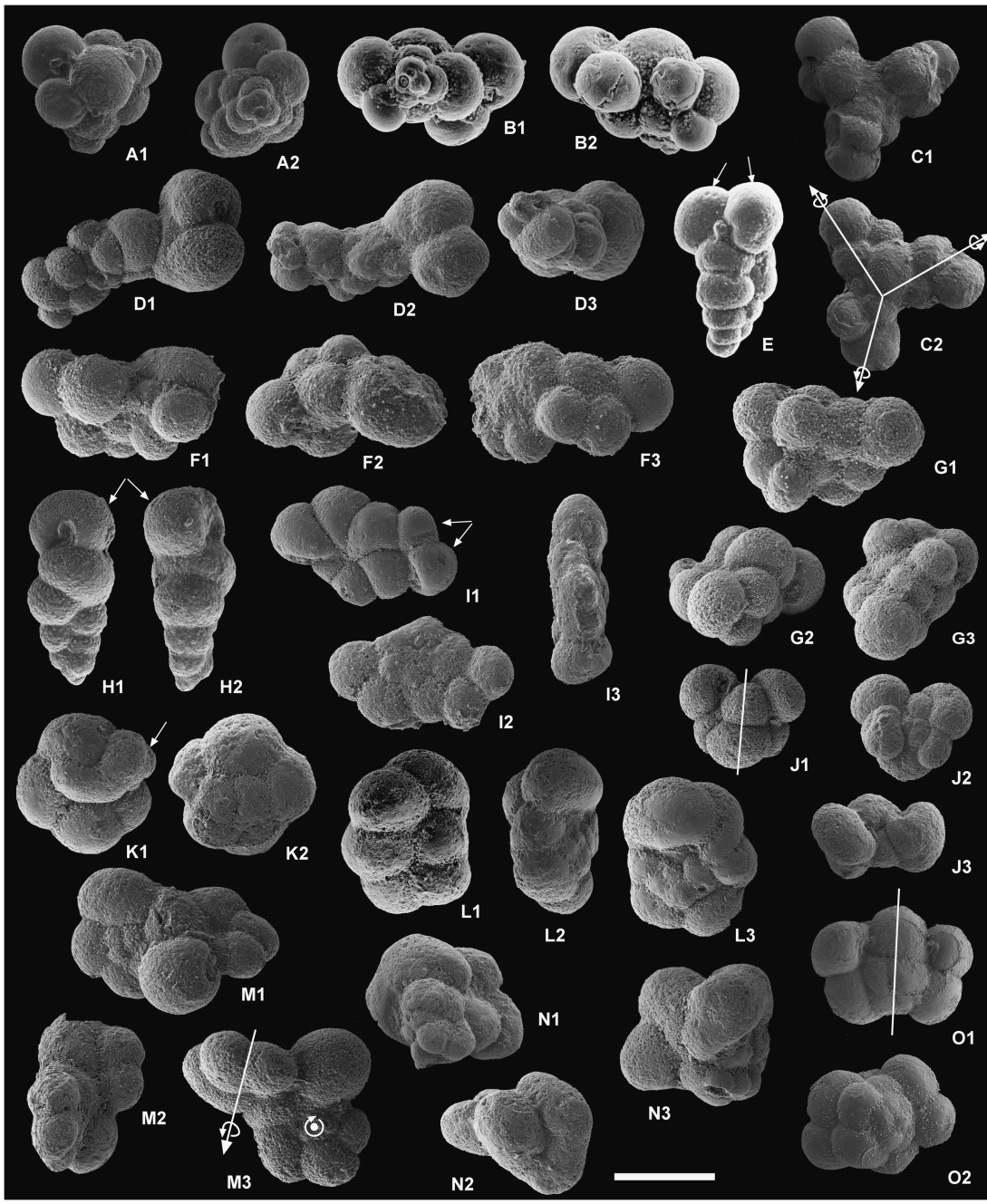

FIGURE 6. Examples of extreme aberrant forms of early Danian planktic foraminifera. Scale bar, 100 microns. A and B, *Guembelitria* spp., multiple ultimate chambers (racemiguembeliform multiserial test). C, *Guembelitria* sp. (probably *G. cretacea*), attached triplets (triamese). D, *Guembelitria* sp. or *Woodringina* sp., general monstrosity (probably attached twins with abnormal, kummerform, and protuberant chambers). E, *W. hornerstownensis*, double or twinned ultimate chambers. F, *Guembelitria* sp. or *Woodringina* sp., general monstrosity (probably attached twins with abnormal chambers). G, *Parvularugoglobigerina* sp. or *Palaeoglobigerina* sp., general monstrosity. H, *W. hornerstownensis*, last chamber in anomalous position, with test going from biserial to uniserial. I, *Pv. longiapertura*, additional chambers and apertures. J, *Palaeoglobigerina* sp. (probably *Pg. luterbacheri*), attached twins (Siamese). K, *Pv. sabina*, bulla-like ultimate chamber. L, *Pv. eugubina*, twisting of entire test (extreme kinking) and overdeveloped last chambers. M, *Parvularugoglobigerina* sp. (probably *Pv. longiapertura*), two specimens with fused tests. N, *Palaeoglobigerina* sp., general monstrosity. O, *Parvularugoglobigerina* sp.; additional chambers and apertures. All specimens come from El Kef, except for some from Aïn Settara (E, F).

https://doi.org/10.1017/pab.2018.16 Published online by Cambridge University Press

chambers can generate monstrous abnormalities. Montgomery (1990) proposed that monstrosities are probably crushed and repaired specimens resulting from extremely stressful shifts in their environment or increased predation by organisms such as copepods.

Paleoenvironmental and Evolutionary Implications

Uppermost Maastrichtian Evolutionary Stability in Open-Ocean Assemblages.—According to Keller et al. (2011), Font et al. (2016), and Punekar et al. (2016), the main eruptive phase (phase 2) of the Deccan Traps may have been concentrated during the last ~50 or 100 Kyr of the Maastrichtian, triggering a short episode of global cooling—and ocean acidification—as a result of sulfate aerosol particles injected into the stratosphere and increased levels of mercury, an extremely toxic heavy metal. Opportunistic *Guembelitria* blooms have also been identified in the uppermost Maastrichtian, mainly in the shallow-marine environments of Israel, Egypt, Texas, and India, which suggests that the environmental deterioration and extinction began with the Deccan eruptions, several tens of thousands of years before the K/Pg boundary (Punekar et al. 2014; Keller et al. 2016). However, only minor *Guembelitria* blooms are present in the deep-marine environments of the Maastrichtian (Pardo and Keller 2008; Punekar et al. 2014). As proposed for warming episodes in the early Danian, *Guembelitria* acmes in shallow neritic environments could have also been under an orbital control related with small variations in sea level, temperature, acidity, and nutrients due to Milankovitch cycles (Quillévéré et al. 2008; Coccioni et al. 2010).

To test the hypothesis that the main eruptive phase (phase 2) of the Deccan Traps may have been concentrated during the last ~50 or 100 Kyr of the Maastrichtian, we have for the first time appraised the rate of aberrant planktic foraminifera in the upper part of the *P. hantkeninoides* Subzone from El Kef and Aïn Settara, as a proxy for ecological stress episodes. Our results indicate that there was a low frequency of aberrants (generally <2.5%) across this interval (Tables 1, 2), similar to the levels recorded in recent deep-ocean sediments under "normal" environmental conditions and reflecting the natural background number of malformations among planktic foraminifers (Mancin and Darling 2015). Low extinction and speciation rates, as well as low volatility and taxonomic flux fluctuations (Figs. 2 and 8), corroborate the high evolutionary stability that prevailed during the latest Maastrichtian in El Kef.

Proliferation of Aberrant Planktic Foraminifera, Chemical Pollution, and Global Warming during the Earliest Danian.—The causes proposed to explain the abnormalities in planktic foraminiferal tests are still very vague, including biological factors (such as unusually high levels of intraspecific variability) or various chemical and physical stressors (see Mancin and Darling 2015). For example, Coccioni and Luciani (2006) speculated that blooms of aberrant *G. irregularis* across the K/Pg boundary are explained as the result of rapid and extreme fluctuations in climate and sea level, as well as intense volcanism and meteoritic impact events, which could have stressed surface waters. The higher values in the FAI identified here during the first 200 Kyr of the Danian (affecting not only *G. irregularis* but all the planktic foraminiferal groups), however, require a better understanding of how the long-term effects of the Chicxulub impact or the paleoenvironmental changes induced by the Deccan eruptions affected planktic foraminiferal assemblages during the early Danian.

Model calculations have suggested several short-term (hour- to decade-long) environmental perturbations caused by the Chicxulub impact (see reviews in Kring 2007; Schulte et al. 2010; Brugger et al. 2017; Artemieva et al. 2017). These include a global pulse of increased thermal radiation on the ground and wildfires caused by the atmospheric re-entry of the ejecta spherules, the production of acid rain, and an injection of dust and aerosol particles into the atmosphere, blocking the sunlight. Using TEX_{86} paleothermometry, a short-term cooling (or "impact winter" phase) during the first months to decades following the Chicxulub impact has been documented at the Brazos River section

https://doi.org/10.1017/pab.2018.16 Published online by Cambridge University Press

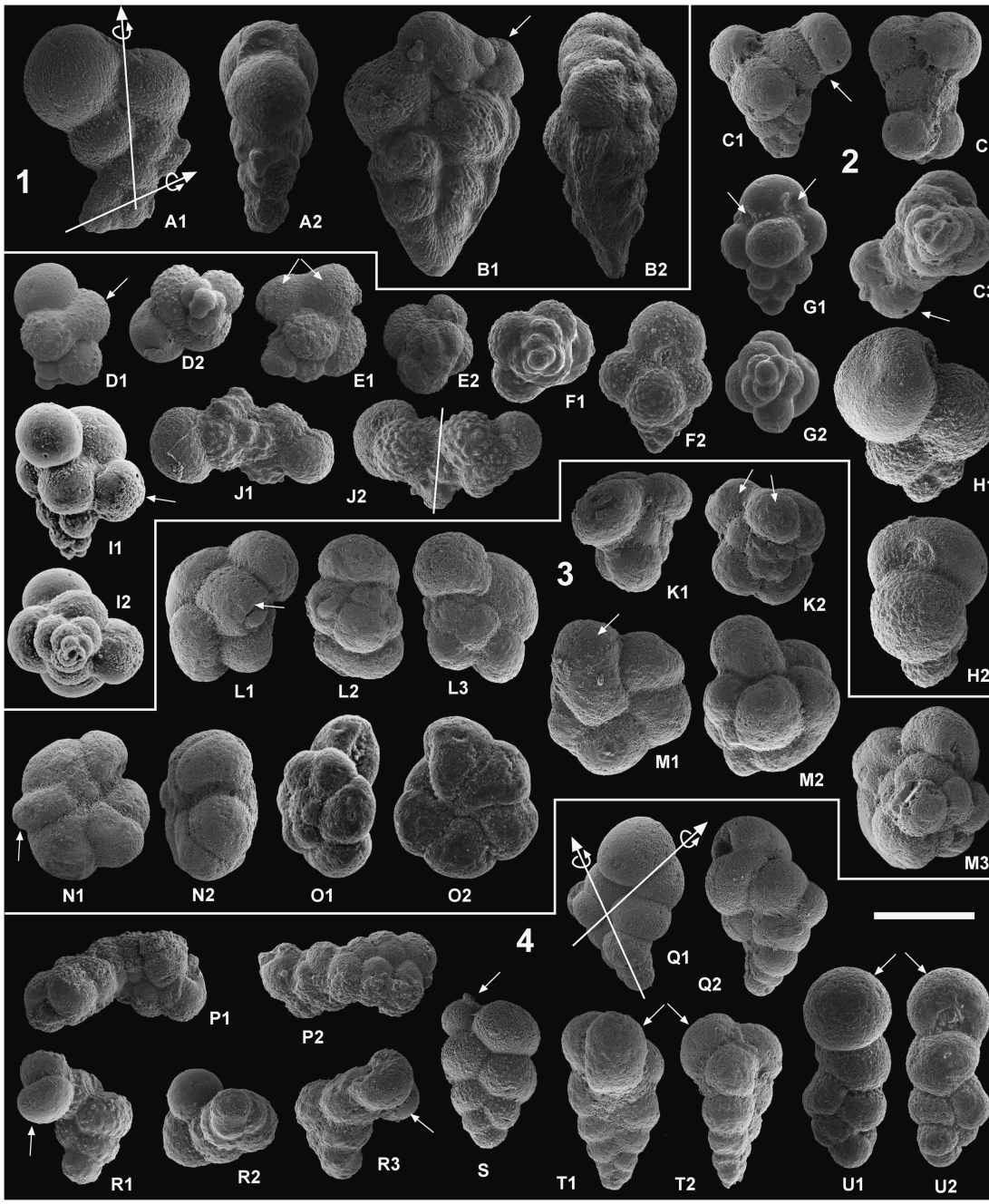

FIGURE 7. Examples of aberrant planktic foraminifera ordered by time intervals and environmental and evolutionary episodes. Scale bar, 100 microns. 1. Latest Maastrichtian: A, *Heterohelix globulosa*, kinking with change in the coiling direction. B, *Pseudoguembelina kempensis*, with multiple ultimate chambers. 2. PFAS-1 and transition between PFAS-1 and PFAS-2: C, *Guembelitria* sp. (probably *G. cretacea*), protuberant chambers. D and E, *Guembelitria* sp. (probably *G. cretacea*), welded chambers. F, *Guembelitria* sp. (probably *G. cretacea*), tetraserial form. G, *Guembelitria* sp. (probably *G. cretacea*), tetraserial form with multiple apertures. H, *W. claytonensis*, abnormal test with overdeveloped or inflated chambers. I, *Guembelitria* sp., multiple ultimate chambers (racemiguembeliform multiserial test). J, *Chiloguembelitria* sp. (probably *Chg. trilobata*), attached twins (Siamese). 3. PFAS-2: K, *Pg. luterbacheri*, double twinned chambers. L, *Pv. sabina*, bulla-like ultimate chamber. M, *Parvularugoglobigerina* sp., bulla-like ultimate chamber. N, *Pv. eugubina*, protuberant aberrant chamber. O, *Pv. longiapertura*, abnormally spiroconvex test. 4. Lower part of PFAS-3 (*Chiloguembelitria* acme): P, *W. claytonensis*?, general monstrosities, probably attached twins (Siamese) with abnormal

https://doi.org/10.1017/pab.2018.16 Published online by Cambridge University Press

in Texas (Vellekoop et al. 2014). Short-term global perturbations were likely major lethal factors for planktic foraminifera in the K/Pg mass extinction event (lasting months or a few years), but are insufficient to account for the increase of aberrants identified in the first 200 Kyr of the Danian.

Increased teratological forms in recent foraminifera are usually related with highly polluted areas (e.g., Alve 1991; Yanko et al. 1998; Geslin et al. 2002; Martin and Nesbitt 2015). Under the effect of extreme poisoning by heavy metals, the ability of foraminifera to constrain the shape of their shells is limited, leading to aberrant morphologies (Caron et al. 1987). The action of toxic heavy metals must have been very intense immediately after the Chicxulub impact. According to Erickson and Dickson (1987), a hypothetical 10-km-diameter chondritic impactor such as that of Chicxulub contains a mass of heavy metals, such as cobalt, nickel, copper, and mercury, comparable to or larger than the world ocean burden. Several heavy metals have relatively inefficient removal mechanisms, such as copper and nickel with greater than 1000-yr steady-state oceanic residence times. In addition, the worldwide sediments contaminated with heavy metals from the Chicxulub impact site may well have been eroded, removed, and resuspended in oceans for several thousand years (Smit and Romein 1985; Smit et al. 1996). Premovic et al. (2008) suggested that humics enriched in heavy metals were transported mainly by fluvial means into the ocean and deposited in the dark-clay bed. Enhanced levels of toxic heavy metals (e.g., nickel, zinc, chromium, cobalt, or copper) have been identified in the dark-clay bed, that is, in the first 10 Kyr after the K/Pg boundary, at Caravaca (Smit and ten Kate 1982), Aïn Settara (Dupuis et al. 2001), and Stevns Klint, Denmark (Premovic et al. 2008).

Chicxulub impact–linked chemical pollution could therefore be a major cause of the first bloom of aberrant planktic foraminifers within the dark-clay bed. In addition, the large amount of CO_2 gas devolatilized in the Chicxulub impact and the collapse of ocean productivity and the biological pump initiated intense global warming through the greenhouse effect after the post-impact winter phase (Kawaragi et al. 2009), persisting as another ecological stress factor for thousands of years. Isotopic data from El Kef indicate a sudden negative excursion in bulk-sediment $\delta^{13}C$ and $\delta^{18}O$ after the K/Pg boundary (Keller and Lindinger 1989), suggesting a warming episode and a decrease in biological productivity at the time of the dark-clay bed deposition and PFAS-1. According to the GTS12 and the biochronological scale of Arenillas et al. (2004), this negative $\delta^{13}C$ excursion lasted for the first 20–25 Kyr of the Danian.

Another potential cause of the first peak of aberrant planktic foraminifers in PFAS-1 could be phytoplankton blooms concentrating toxins in the surface waters (Jiang et al. 2010; Schueth et al. 2015). Toxicity is a well-known product of modern plankton blooms (Castle and Rodgers 2009), and geographically heterogeneous spikes of phytoplankton groups are reported in the earliest Danian. For example, quantitative analyses with organic-walled marine dinoflagellate cyst assemblages in the lowermost Danian of El Kef show a relevant acme of the *Andalusiella–Palaeocystodinium* complex between 10 and 15 cm above the K/Pg boundary (Brinkhuis et al. 1998). This peak correlates approximately with the initial increase in aberrant tests of planktic foraminifera at El Kef, but not with the maximum values recorded between 37 and 97 cm above the K/Pg boundary (Fig. 3, Table 1). Although phytoplankton blooms may have favored the concentration of toxins in the surface-water layers, more studies are needed to establish the relationship between such blooms and

chambers. Q, *W. hornerstownensis*, kinking with change in the coiling direction. R, *W. claytonensis*, kinking with change in the coiling direction and last chambers apparently protuberant. S, *W. claytonensis*, reduced last chamber (kummerform). T, *Ch. taurica*, last chamber in anomalous position, with test going from biserial to triserial. U, *W. claytonensis*, last chamber in anomalous position, with test going from biserial to uniserial. Most of the specimens come from El Kef, and the rest are from Aïn Settara (F, P, Q), Elles (G, K), Agost (O), and Caravaca (T).

https://doi.org/10.1017/pab.2018.16 Published online by Cambridge University Press

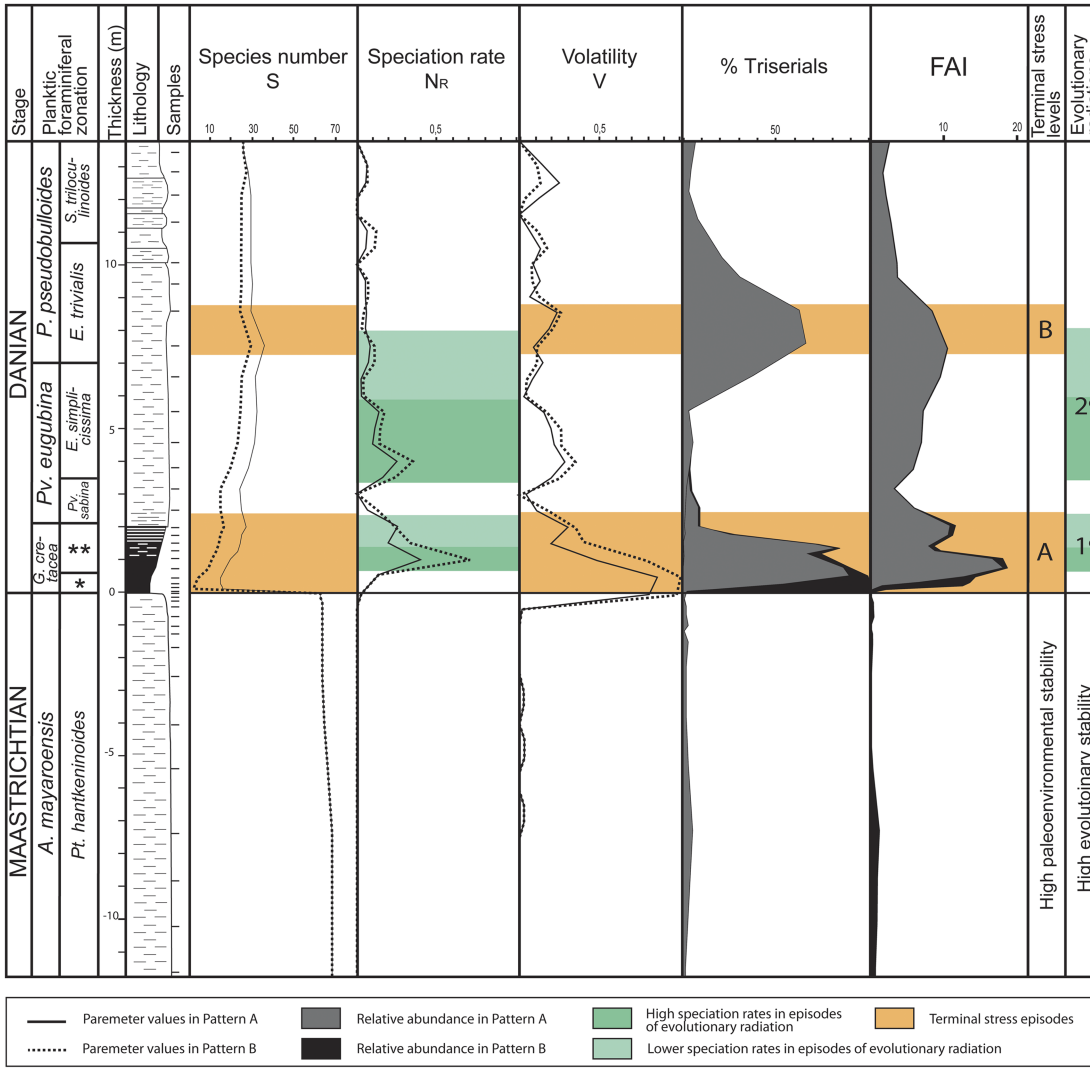

FIGURE 8. Shifts in specific richness (species number), speciation rate and volatility (according to the model of Dean and McKinney, 2001), relative abundance (%) of triserial specimens, and FAI (rate of aberrants in %) across the K/Pg boundary at El Kef; solid line and gray shading: hypothesis of pattern A; dotted line and black shading: hypothesis of pattern B; orange shading: terminal stress levels according to the model of Weinkauf et al. (2014), A corresponding to PFAS-1 and B to the *Chiloguembelitria* acme; green shading, evolutionary radiations, with shading in dark green to indicate high speciation rates (see online version for color). FAI, Foraminiferal Abnormality Index (% aberrant planktic foraminifera). **Mh. holmdelensis* Subzone (= Zone P0); ***Pv. longiapertura* Subzone.

the proliferations of aberrant planktic foraminiferal tests in the early Danian. In any case, spikes of *Andalusiella–Palaeocystodinium* complex and other groups (such as the calcareous dinoflagellate cyst *Thoracosphaera* spp. or the nannofossil species *Braarudosphaera bigelowii*) identified in the Tethyan realm are usually explained as blooms of opportunistic taxa related to long-term environmental effects of the Chicxulub impact (Lamolda et al. 2005; Vellekoop et al. 2015).

On the basis of several independent stratigraphic, geochronological, geochemical, and tectonic constraints, Richards et al. (2015) hypothesized that the main Deccan eruptive phase (phase 2, >70% of the lava flows) could have been triggered by the Chicxulub impact during a relatively brief time interval on the order of one to several hundred thousand years. If this hypothesis by Richards et al. (2015) is correct, the long-term disruptive

https://doi.org/10.1017/pab.2018.16 Published online by Cambridge University Press

effects of the Chicxulub impact could be combined in the early Danian with those of Deccan volcanism, including a chemical contamination of the ocean surface over a longer period of time. This hypothesis could explain why the values of the FAI at the El Kef and Aïn Settara sections remained high during at least the first 200 Kyr after the Chicxulub impact (including the interval PFAS-2).

As mentioned earlier, the second increase in aberrant forms coincides with the *Chiloguembelitria* bloom in the lower part of PFAS-3 (Figs. 3, 8). This episode spanned between approximately 70 and 200 Kyr after the K/Pg boundary, so it cannot be related to the long-term disruptive effects of the Chicxulub impact. On the contrary, it seems that it was caused by another independent, later period of intense ecological stress perhaps linked to the Deccan eruptions (phase 2 or 3). Quillévéré et al. (2008) recognized in the lower Danian (in the *E. trivialis* Subzone, or Subzone P1a) a warming episode called Dan-C2 (the first hyperthermal episode of the Paleogene), which lasted approximately 100 Kyr. Although Dan-C2 and similar episodes could be a result of orbital cycles, Coccioni et al. (2010) proposed a possible link between this warming episode and the Deccan volcanism. According to this scenario, the second increase of the FAI, the *Chiloguembelitria* bloom, and the Dan-C2 episode could therefore be related. The low values of the FAI after the *Chiloguembelitria* bloom (in the *S. triloculinoides* Subzone, or Subzone P1b) suggest a period of greater environmental stability. This interval is widely dominated by biserial *Woodringina* and *Chiloguembelina*, typical of the PFAS-3 episode. Nevertheless, Coccioni et al. (2010) suggested that the predominance of biserials in Gubbio, along with other micropaleontological and geochemical proxies, was indicative of stressed ecological conditions (climatic warming and low oxygenation and acidification of ocean waters) during the Dan-C2 episode. According to this scenario, the whole PFAS-3 episode could be a record of the late eruptions of Deccan phase 2 or the first eruptions of phase 3. Moreover, the *Chiloguembelitria* bloom in the lower part of PFAS-3 could be the result of a more intense volcanic pulse during Dan-C2, though not one recorded at Gubbio by Coccioni et al. (2010).

Evolutionary Implications.—Weinkauf et al. (2014) suggested that the phenotypic history of planktic foraminiferal assemblages allows the detection of threshold levels of ecological stress episodes that are likely to lead to extinction. According to these authors, an increase in interspecific morphological variability and abnormal forms can be observed at terminal stress levels immediately before extinction, indicating disruptive selection. In contrast, in periods of environmental stability and non-terminal stress levels, a decrease in morphological variability and abnormal forms is recognized, indicating stabilizing selection.

If the hypothesis that the massive eruptions of Deccan phase 2 were concentrated in the last 50 or 100 Kyr of the Maastrichtian and started a gradual mass extinction in planktic foraminifera before the K/Pg boundary (Punekar et al. 2016) is correct, a terminal stress episode with abundant aberrant forms should have been recorded below the K/Pg extinction horizon at El Kef and Aïn Settara. However, there is no evidence for such a scenario and, as in many sections worldwide, most Maastrichtian species suddenly become extinct at the K/Pg boundary following a catastrophic extinction pattern compatible with the short-term effects of the Chicxulub impact (Smit 1982, 1990; Huber 1996; Arz et al. 2000; Arenillas et al. 2000a,b; Huber et al. 2002; Molina et al. 2005; Gallala 2014). Similarly, latest Maastrichtian climatic fluctuations and environmental perturbations linked to Deccan volcanism had a relatively weak impact on the diversity of the calcareous nannoplankton assemblages before the K/Pg boundary, as evidenced in Elles and other sections worldwide (Thibault et al. 2016).

The first bloom of aberrants and PFAS-1 in the earliest Danian occurred in an interval in which the speciation rate was very high, especially in the lower part of the *Pv. longiapertura* Subzone, which also shows high volatility and relevant fluctuations in the taxonomic flux (Figs. 2 and 8). Arenillas et al. (2016) suggested that the speciation rate may have been increased in response to the long-term meteoritic pollution of the oceans, which may have caused increased mutation rates for at

https://doi.org/10.1017/pab.2018.16 Published online by Cambridge University Press

least 10 to 20 Kyr after the K/Pg boundary and triggered the first evolutionary radiation of planktic foraminifera. Many mutations in planktic foraminifera are likely to have been lethal, causing mortality before the adult stage was reached. However, genetic mutations could have accelerated the evolution of planktic foraminifera in the early Danian, being amplified as a consequence of stressed and adverse environments (BouDagher-Fadel 2012). In addition, many other mutations would have been deleterious, producing malformations and teratological forms, as has been proposed for recent foraminifera (e.g., Mancin and Darling 2015). The high values of the FAI identified in the dark-clay bed and PFAS-1 at El Kef and Aïn Settara are consistent with this hypothesis. This interval occurred during the survival and recovery phases after the K/Pg boundary extinction according to the terminology of Kauffman and Erwin (1995), in which *Guembelitria* included the "disaster species" and the minute parvularugoglobigerinids the "progenitor species" (Molina 2015), although the latter had a benthic origin, as has recently been proposed by Arenillas and Arz (2017). The evolutionary history of the planktic foraminifera was restarted almost from scratch after the K/Pg boundary extinction, suggesting that all the latest Maastrichtian species went extinct at the K/Pg boundary, except for some species of *Guembelitria* (see also Smit 1982; Arenillas et al. 2016).

The second bloom of aberrants and the *Chiloguembelitria* acme appear to be better adjusted to a terminal stress episode, as proposed by Weinkauf et al. (2014). Nonterminal stress episodes could correspond to PFAS-2, dominated by parvularugoglobigerinids and characterized by an aberrant rate lower than in PFAS-1 and the *Chiloguembelitria* acme. It is not possible to speak of environmental stability in PFAS-2, because values of the FAI and volatility remain high. In fact, the speciation rate in the upper part of PFAS-2 is high (Fig. 8) as a consequence of the beginning of the second evolutionary radiation. Nevertheless, the maximum in species richness (S = species number) of the early Danian is reached during the beginning of the *Chiloguembelitria* acme (Fig. 8), which represents a terminal stress episode. This is because the species that emerged during the first and second evolutionary radiations overlapped in time (Fig. 1). The parvularugoglobigerinids, which appeared in the first radiation, went extinct toward the end of the *Chiloguembelitria* acme, increasing the extinction rate (Fig. 8). Parvularugoglobigerinids were replaced definitively by the more ornamented, larger trochospiral species of the second evolutionary radiation. In this case, the *Chiloguembelitria* included the disaster species, and the species that appeared in the second radiation (those of *Eoglobigerina*, *Parasubbotina*, *Globanomalina*, and *Praemurica*, among others) were the progenitor species.

Conclusions

1. A high-resolution, quantitative biostratigraphic study across the K/Pg boundary from open-ocean Tunisian sections (El Kef and Aïn Settara) revealed a proliferation of aberrant planktic foraminifera during approximately the first 200 Kyr of the Danian. Various categories and types of abnormalities were identified, including abnormal tests, extra chambers, attached twin tests, and general monstrosities.

2. The proliferation of aberrants occurred in two main pulses. The first was more intense and occurred during the first 20 to 25 Kyr after the K/Pg boundary, spanning the dark-clay bed. It is characterized by abnormal forms of triserials (*Guembelitria*), but also of parvularugoglobigerinids (*Parvularugoglobigerina* and *Palaeoglobigerina*) from just the first evolutionary radiation of Danian planktic foraminifera. The second pulse is recorded between approximately 70 and 200 Kyr after the K/Pg boundary and is characterized mainly by abnormal forms of triserials (*Chiloguembelitria*) and biserials (*Woodringina* and *Chiloguembelina*).

3. These two pulses of aberrants correlate respectively with the *Guembelitria* acme in PFAS-1 and the dark-clay bed and with the *Chiloguembelitria* acme in the lower part of PFAS-3, both of which have been interpreted as ecological stress episodes. The FAI during the parvularugoglobigerinid acme in PFAS-2 is lower, but remains high enough to suggest that environmental conditions were also unstable during this interval, in which the second evolutionary radiation of Danian planktic foraminifera occurred.

https://doi.org/10.1017/pab.2018.16 Published online by Cambridge University Press

4. According to the data set available here, the high values of the FAI in PFAS-1 seems to be more related to long-term environmental effects of the Chicxulub impact. By contrast, the second bloom of aberrants during the *Chiloguembelitria* acme was caused by an independent, later period of ecological stress perhaps linked to the Deccan eruptions.

5. The absence of an ecological stress episode rich in abnormal tests during the latest Maastrichtian in both the El Kef and Aïn Settara locations, as well as the high values of the FAI during the first 200 Kyr of the Danian, could be compatible with the hypothesis that the Chicxulub impact triggered the main phase of the Deccan Traps. This would render the Deccan volcanism an unlikely candidate as the cause of the K/Pg boundary mass extinction.

Acknowledgments

We thank I. Polovodova, C. M. Lowery, and two anonymous reviewers for their comments and critiques, which have greatly helped improve this paper. This study is a contribution to project CGL2015-64422-P (MINECO/FEDER-UE) and is also partially supported by the Departamento de Educación y Ciencia of the Aragonian Government, cofinanced by the European Social Fund (grant number DGA group E05). V.G. acknowledges support from the Spanish Ministerio de Economía, Industria y Competitividad (FPI grant BES-2016-077800). The authors would like to acknowledge the use of the Servicio General de Apoyo a la Investigación-SAI, Universidad de Zaragoza. The authors are grateful to Rupert Glasgow for improvement of the English text.

Literature Cited

Alegret, L., E. Thomas, and K. C. Lohmann. 2012. End-Cretaceous marine mass extinction not caused by productivity collapse. Proceedings of the National Academy of Sciences USA 109:728–732.

Alvarez, L. W., W. Alvarez, F. Asaro, and H. V. Michel. 1980. Extraterrestrial cause for the Cretaceous–Tertiary extinction. Science 208:1095–1108.

Alvarez, W., J. Smit, W. Lowrie, F. Asaro, S. V. Margolis, P. Claeys, M. Kastner, and A. R. Hildebrand. 1992. Proximal impact deposits at the Cretaceous–Tertiary boundary in the Gulf of Mexico: a restudy of DSDP Leg 77 Sites 536 and 540. Geology 20:697–700.

Alve, E. 1991. Benthic foraminifera in sediment cores reflecting heavy metal pollution in Soerfjord, Western Norway. Journal of Foraminiferal Research 21:1–19.

Apellaniz, E., X. Orue-Etxebarría, and H. P. Luterbacher. 2002. Evolution of the early Paleocene planktonic foraminifera: a Basque point of view. Neues Jahrbuch für Geologie und Paläontologie, Abhundlungen 225:157–194.

Arenillas, I., and J. A. Arz. 2017. Benthic origin and earliest evolution of the first planktonic foraminifera after the Cretaceous/Paleogene boundary mass extinction. Historical. Biology 29:17–24.

Arenillas, I., J. A. Arz, E. Molina, and C. Dupuis. 2000a. The Cretaceous/Paleogene (K/P) boundary at Aïn Settara, Tunisia: sudden catastrophic mass extinction in planktic foraminifera. Journal of Foraminiferal Research 30:202–218.

——. 2000b. An independent test of planktonic foraminiferal turnover across the Cretaceous/Paleogene (K/P) boundary at El Kef, Tunisia: catastrophic mass extinction and possible survivorship. Micropaleontology 46:31–49.

Arenillas, I., J. A. Arz, and E. Molina. 2002. Quantifying the evolutionary turnover across the K/T boundary catastrophic planktic foraminiferal extinction event at El Kef, Tunisia. Geologiska Föreningens Förhandlingen 124:121–126.

——. 2004. A new high-resolution planktonic foraminiferal zonation and subzonation for the lower Danian. Lethaia 37:79–95.

Arenillas, I., J. A. Arz, J. M. Grajales-Nishimura, G. Murillo-Muñetón, W. Alvarez, A. Camargo-Zanoguera, E. Molina, and C. Rosales-Domínguez. 2006. Chicxulub impact event is Cretaceous/Paleogene boundary in age: new micropaleontological evidence. Earth and Planetary Science Letters 249:241–257.

Arenillas, I., J. A. Arz, J. M. Grajales-Nishimura, A. Meléndez, and R. Rojas-Consuegra. 2016. The Chicxulub impact is synchronous with the planktonic foraminifera mass extinction at the Cretaceous/Paleogene boundary: new evidence from the Moncada section, Cuba. Geologica Acta 14:35–51.

Arenillas, I., J. A. Arz, and V. Gilabert. 2017. Revalidation of the genus *Chiloguembelitria* Hofker: implications for the evolution of early Danian planktonic foraminifera. Journal of African Earth Sciences 134:435–456.

Artemieva, N., and J. Morgan, Expedition 364 Science Party 2017). Quantifying the release of climate-active gases by large meteorite impacts with a case study of Chicxulub. Geophysical Research Letters 44. doi: 10.1002/2017GL074879.

Arz, J. A., I. Arenillas, E. Molina, and R. Sepúlveda. 2000. La estabilidad faunística de foraminíferos planctónicos en el Maastrichtiense superior y su extinción en masa catastrófica en el límite K/T de Caravaca, España [The faunistic stability of planktonic foraminifera in the Upper Maastrichtian and their catastrophic mass extinction at the K/T boundary of Caravaca, Spain]. Revista Geológica de Chile 27:27–47.

Arz, J. A., I. Arenillas, and C. Náñez. 2010. Morphostatistical analysis of Maastrichtian populations of *Guembelitria* from El Kef, Tunisia. Journal of Foraminiferal Research 40:148–164.

Aze, T., T. H. G. Ezard, A. Purvis, H. Coxall, D. R. M. Stewart, B. S. Wade, and P. N. Pearson. 2011. A phylogeny of Cenozoic macroperforate planktonic foraminifera from fossil data. Biological Reviews 86:900–927.

Ballent, S. C., and A. P. Carignano. 2008. Morphological abnormalities in Late Cretaceous and early Paleocene foraminifer tests (northern Patagonia, Argentina). Marine Micropaleontology 67:288–296.

Bardeen, C. G., R. R. Garcia, O. B. Toon, and A. J. Conley. 2017. On transient climate change at the Cretaceous – Paleogene boundary due to atmospheric soot injections. Proceedings of the National Academy of Sciences USA 114:E7415–E7424.

Berggren, W. A., and P. N. Pearson. 2005. A revised tropical to subtropical Paleogene planktonic foraminiferal zonation. Journal of Foraminiferal Research 35:279–298.

Bijma, J., C. Hemleben, H. Oberhänsli, and M. Spindler. 1992. The effect of increased water fertility on tropical spinose planktonic

https://doi.org/10.1017/pab.2018.16 Published online by Cambridge University Press

foraminifers in laboratory cultures. Journal of Foraminiferal Research 22:242–256.
Birch, H.S., H. K. Coxall, P. N. Pearson, D. Kroon, and D. N. Schmidt. 2016. Partial collapse of the marine carbon pump after the Cretaceous–Paleogene boundary. Geology 44:287–290.
Boltovskoy, E., and R. Wright. 1976). Recent Foraminifera. Dr. W. Junk b.v. Publishers, The Hague.
BouDagher-Fadel, M. K. 2012). Biostratigraphic and geological significance of planktonic foraminifera, 1st ed. Developments in Palaeontology and Stratigraphy 22:1–289. Elsevier, Amsterdam.
Brinkhuis, H., and W. J. Zachariasse. 1988. Dinoflagellate cyst, sea level changes and planktonic foraminifers across the Cretaceous–Tertiary boundary at El Haria, Northwest Tunisia. Marine Micropaleontology 13:153–191.
Brinkhuis, H., J. P. Bujak, J. Smit, G. J. M. Versteegh, and H. Visscher. 1998. Dinoflagellate-based sea surface temperature reconstructions across the Cretaceous–Tertiary boundary. Palaeogeography, Palaeoclimatology, Palaeoecology 141:67–83.
Brugger, J., G. Feulner, and S. Petri. 2017). Baby, it's cold outside: climate model simulations of the effects of the asteroid impact at the end of the Cretaceous. Geophysical Research Letters 44. doi: 10.1002/2016GL072241.
Caron, D. A., J. W. F. Faber, and A. W. H. Bé. 1987. Growth of the spinose planktonic foraminifer *Orbulina universa* in laboratory culture and the effect of temperature on life processes. Journal of Marine Biological Association of the United Kingdom 67:343–358.
Castle, J. W., and J. H. Rodgers, Jr. 2009. Hypothesis for the role of toxin-producing algae in Phanerozoic mass extinctions based on evidence from the geologic record and modern environments. Environmental Geosciences 16:1–23.
Chenet, A.-L., X. Auidelleur, F. Fluteau, V. Y. Courtillot, and S. Bajpai. 2007. ^{40}K-^{40}Ar dating of the main Deccan large igneous province: further evidence of KTB age and short duration. Earth and Planetary Science Letters 263:1–15.
Chenet, A.-L., V. Courtillot, F. Fluteau, M. Gérard, X. Quidelleur, S. F. R. Khadri, K. V. Subbarao, and T. Thordarson. 2009. Determination of rapid Deccan eruptions across the Cretaceous–Tertiary boundary using paleomagnetic secular variation. 2. Constraints from analysis of eight new sections and synthesis for a 3500-m-thick composite section. Journal of Geophysical Research 114:B06103.
Coccioni, R., and V. Luciani. 2006. *Guembelitria irregularis* bloom at the K-T boundary: morphological abnormalities induced by impact-related extreme environmental stress?. Pp. 179–196. *in* C. Cockell, C. Koeberl, and I. Gilmour, eds. Biological processes associated with impact events. Springer, Berlin.
Coccioni, R., F. Frontalini, G. Bancalà, E. Fornaciari, L. Jovane, and M. Sprovieri. 2010. The Dan-C2 hyperthermal event at Gubbio (Italy): global implications, environmental effects, and cause(s). Earth and Planetary Science Letters 297:298–305.
Courtillot, V. E., G. Feraud, H. Maluski, D. Vandamme, M. G. Moreau, and J. Besse. 1988. Deccan flood basalts and the Cretaceous/Tertiary boundary. Nature 333:843–846.
Coxall, H. K., S. L. D'Hondt, and J. C. Zachos. 2006. Pelagic ecosystem recovery after the K-T mass extinction. Geology 34:297–300.
Dean, W. G., and M. L. McKinney. 2001. Taxonomic flux as a measure of evolutionary turnover. Revista Española de Paleontología 16:29–38.
D'Hondt, S. 2005. Consequences of the Cretaceous/Paleogene mass extinction for marine ecosystems. Annual Review of Ecology, Evolution and Systematics 36:295–317.
D'Hondt, S., P. Donaghay, J. C. Zachos, D. Luttenberg, and M. Lindinger. 1998. Organic carbon fluxes and ecological recovery from the Cretaceous–Tertiary mass extinction. Science 282:276–279.
Dupuis, C., E. Steurbaut, E. Molina, R. Rauscher, N. P. Tribovillard, I. Arenillas, J. A. Arz, F. Robaszynski, M. Caron, E. Robin, ;R. Rocchia, and I. Lefèvre. 2001. The Cretaceous–Paleogene (K/P) boundary in the Aïn Settara section (Kalaat-Senan, Central Tunisia): lithological, micropaleontological and geochemical evidence. Bulletin de l'Institut Royal des Sciences Naturelles de Belgique 71:169–190.
Erickson, D. J., and S. M. Dickson. 1987. Global trace-element biogeochemistry at the K/T boundary—oceanic and biotic response to a hypothetical meteorite impact. Geology 15:1014–1017.
Font, E., T. Adatte, A. N. Sial, A. D. de Lacerda, G. Keller, and J. P. Punekar. 2016. Mercury anomaly, Deccan volcanism, and the end-Cretaceous mass extinction. Geology 44:171–174.
Frontalini, F., and R. Coccioni. 2008. Benthic foraminifera for heavy metal pollution monitoring: a case study from the central Adriatic Sea coast of Italy. Estuarine, Coastal and Shelf Science 76:404–427.
Gallala, N. 2014. Biostratigraphie, paleoecology et zones d'acmé des foraminiferres planctoniques au passage Crétacé-Paleogène dans la Téthys (Tunisie et Espagne) et l'Atlantique (France). [Biostratigraphy, paleoecology and acme-zones of planktic foraminifera of the Cretaceous/Paleogene transition in the Tethys (Tunisia and Spain) and the Atlantic realm (France)]. Annales de Paléontologie 100:193–215.
Gerasimov, M. V. 2002. Toxins produced by meteorite impacts and their possible role in a biotic mass extinction. Geological Society of America Special Paper 356:705–717.
Gerstel, J., R. Thunell, R. C. Zachos, and M. A. Arthur. 1986. The Cretaceous–Tertiary boundary event in the North Pacific; planktonic foraminiferal results from the Deep Sea Drilling Project 577, Shatsky Rise. Paleoceanography 1:97–117.
Geslin, E., J. P. Debenay, W. Duleba, and C. Bonetti. 2002. Morphological abnormalities of foraminiferal tests in Brazilian environments: comparison between polluted and non-polluted areas. Marine Micropaleontology 45:151–168.
Gradstein, F. M., J. G. Ogg, M. Schmitz, and G. Ogg eds. 2012. The geologic time scale 2012. Elsevier, Amsterdam.
Hecht, A. D., and S. M. Savin. 1972. Phenotypic variation and oxygen isotope ratios in Recent planktonic foraminifera. Journal of Foraminiferal Research 2:55–67.
Hildebrand, A. R., G. T. Penfield, D. A. Kring, M. Pilkington, A. Camargo, S. B. Jacobsen, and W. V. Boynton. 1991. Chicxulub crater: a possible Cretaceous/Tertiary boundary impact crater on the Yucatan Peninsula, Mexico. Geology 19:867–871.
Hofker, J. 1978. Analysis of a large succession of samples through the Upper Maastrichtian and the Lower Tertiary of Drill Hole 47.2, Shatsky Rise, Pacific, Deep Sea Drilling Project. Journal of Foraminiferal Research 8:46–75.
Hollis, C. J., K. A. Rodgers, C. P. Strong, B. D. Field, and K. M. Rogers. 2003. Paleoenvironmental changes across the Cretaceous/Tertiary boundary in the northern Clarence valley, southeastern Marlborough, New Zealand. New Zealand Journal of Geology and Geophysics 46:209–234.
Hsü, K. J., and J. A. McKenzie. 1985. "Strangelove" ocean in the earliest Tertiary. American Geophysical Union, Geophysical Monograph Series 32:487–892.
Huber, B. T. 1996. Evidence for planktonic foraminifer reworking versus survivorship across the Cretaceous–Tertiary boundary at high latitudes. Geological Society of America Special Paper 307:319–334.
Huber, B. T., K. G. MacLeod, and R. Norris. 2002. Abrupt extinction and subsequent reworking of Cretaceous planktonic foraminifera across the Cretaceous/Tertiary boundary: evidence for the subtropical North Atlantic. Geological Society of America Special Paper 356:277–290.
Hull, P. M., and R. D. Norris. 2011. Diverse patterns of ocean export productivity change across the Cretaceous–Paleogene boundary: new insights from biogenic barium. Paleoceanography 26: PA3205. doi: 10.1029/2010PA002082.
Husson, D., B. Galbrun, S. Gardin, and N. Thibault. 2014. Tempo and duration of short-term environmental perturbations across the Cretaceous–Paleogene boundary. Stratigraphy 11:159–171.

Jiang, S., T. J. Bralower, M. E. Patzkowsky, L. R. Kump, and J. D. Schueth. 2010. Geographic controls on nannoplankton extinction across the Cretaceous/Palaeogene boundary. Nature Geoscience 3:280–285.

Kaiho, K., and M. A. Lamolda. 1999. Catastrophic extinction of planktonic foraminifera at the Cretaceous–Tertiary boundary evidenced by stable isotopes and foraminiferal abundance at Caravaca, Spain. Geology 27:355–358.

Kauffman, E. G., and D. H. Erwin. 1995. Surviving mass extinctions. Geotimes 14:14–17.

Kawaragi, K., Y. Sekine, T. Kadono, S. Sugita, S. Ohno, K. Ishibashi, K. Kurosawa, T. Matsui, and S. Ikeda. 2009. Direct measurements of chemical composition of shock-induced gases from calcite: an intense global warming after the Chicxulub impact due to the indirect greenhouse effect of carbon monoxide. Earth and Planetary Science Letters 282:56–64.

Keller, G. 2003. Biotic effects of impacts and volcanism. Earth and Planetary Science Letters 215:249–264.

Keller, G., and S. Abramovich. 2009. Lilliput effect in late Maastrichtian planktic foraminifera. Response to environmental stress. Palaeogeography, Palaeoclimatology, Palaeoecology 284:47–62.

Keller, G., and M. Lindinger. 1989. Stable isotope, TOC and $CaCO_3$, record across the Cretaceous/Tertiary boundary at El Kef, Tunisia. Palaeogeography, Palaeoclimatology, Palaeoecology 73:243–265.

Keller, G., and A. Pardo. 2004. Disaster opportunists Guembelitrinidae—index for environmental catastrophes. Marine Micropaleontology 53:83–116.

Keller, G., P. H. Bhowmick, H. Upadhyay, A. Dave, A. N. Reddy, B. C. Jaiprakash, and T. Adatte. 2011. Deccan volcanism linked to the Cretaceous–Tertiary boundary mass extinction: new evidence from ONGC wells in the Krishna-Godavari basin. Journal Geological Society of India 78:399–428.

Keller, G., P. Mateo, and J. Punekar. 2016. Upheavals during the Late Maastrichtian: volcanism, climate and faunal events preceding the end-Cretaceous mass extinction. Palaeogeography, Palaeoclimatology, Palaeoecology 441:137–151.

Koutsoukos, E. A. M. 2014. Phenotypic plasticity, speciation, and phylogeny in early Danian planktic foraminifera. Journal of Foraminiferal Research 44:109–142.

Kring, D. A. 2007. The Chicxulub impact event and its environmental consequences at the Cretaceous/Tertiary boundary. Palaeogeography, Palaeoclimatology, Palaeoecology 255:4–21.

Lamolda, M., M. C. Melinte, and K. Kaiho. 2005. Nannofloral extinction and survivorship across the K/T boundary at Caravaca, southeastern Spain. Palaeogeography, Palaeoclimatology, Palaeoecology 224:27–52.

Li, L., and G. Keller. 1998. Maastrichtian climate, productivity and faunal turnovers in planktic foraminifera in South Atlantic DSDP sites 525A and 21. Marine Micropaleontology 33:55–86.

Luciani, V., L. Giusberti, C. Agnini, J. Backman, E. Fornaciari, and D. Rio. 2007. The Paleocene–Eocene Thermal Maximum as recorded by Tethyan planktonic foraminifera in the Forada section (northern Italy). Marine Micropaleontology 64:189–214.

Mancin, N., and K. Darling. 2015. Morphological abnormalities of planktonic foraminiferal tests in the SW Pacific Ocean over the last 550 ky. Marine Micropaleontology 120:1–19.

Martin, R. A., and E. A. Nesbitt. 2015. Foraminiferal evidence of sediment toxicity in anthropogenically influenced embayments of Puget Sound, Washington, U.S.A. Marine Micropaleontology 121:97–106.

Molina, E. 2015. Evidence and causes of the main extinction events in the Paleogene based on extinction and survival patterns of foraminifera. Earth-Science Reviews 140:166–181.

Molina, E., L. Alegret, I. Arenillas, and J. A. Arz. 2005. The Cretaceous/Paleogene boundary at the Agost section revisited: paleoenvironmental reconstruction and mass extinction pattern. Journal of Iberian Geology 31:137–150.

Molina, E., L. Alegret, I. Arenillas, J. A. Arz, N. Gallala, J. Hardenbol, K. von Salis, E. Steurbaut, N. Vandenberghe, and D. Zaghbib-Turki. 2006. The Global Stratotype Section and Point of the Danian stage (Paleocene, Paleogene, "Tertiary", Cenozoic) at El Kef, Tunisia: original definition and revision. Episodes 29:263–278.

Molina, E., L. Alegret, I. Arenillas, J. A. Arz, N. Gallala, M. Grajales-Nishimura, G. Murillo-Muñetón, and D. Zaghbib-Turki. 2009. The Global Boundary Stratotype Section and Point for the base of the Danian stage (Paleocene, Paleogene, "Tertiary," Cenozoic): auxiliary sections and correlation. Episodes 32:84–95.

Montgomery, H. 1990. Abnormal terminal Cretaceous foraminifera of east-central Texas. Texas Journal of Science 42:37–44.

Murray, J. W. 2006. Ecology and applications of benthic foraminifera. Cambridge University Press, Cambridge.

Ocampo, A., V. Vajda, and E. Buffetaut. 2006. Unravelling the Cretaceous–Paleogene (KT) turnover: evidence from flora, fauna and geology. Pp. 197–220. *in* C. Cockell, C. Koeberl, and I. Gilmour, eds. Biological processes associated with impact events. Springer, Berlin.

Olsson, R. K., C. Hemleben, W. A. Berggren, and B. T. Huber. 1999. Atlas of Paleocene planktonic Foraminifera. Smithsonian Contributions to Paleobiology. 85:1–252.

Olsson, R. K., J. D. Wright, and K. G. Miller. 2001. Paleobiogeography of *Pseudotextularia elegans* during the latest Maastrictian global warming event. Journal of Foraminiferal Research 31:275–282.

Omaña, L., G. Alencáster, J. R. Torres Hernández, and R. López Doncel. 2012. Morphological abnormalities and dwarfism in Maastrichtian foraminifera from the Cárdenas Formation, Valles-San Luis Potosí Platform, Mexico: evidence of paleoenvironmental stress. Boletín de la Sociedad Geológica Mexicana 64:305–318.

Pardo, A., and G. Keller. 2008. Biotic effects of environmental catastrophes at the end of the Cretaceous and Early Tertiary: *Guembelitria* and *Heterohelix* blooms. Cretaceous Research 29:1058–1073.

Petersen, S. V., A. Dutton, and K. C. Lohmann. 2016. End-Cretaceous extinction in Antarctica linked to both Deccan volcanism and meteorite impact via climate change. Nature. Communications 7:12079.

Polovodova, I., and J. Schönfeld. 2008. Foraminiferal test abnormalities in the western Baltic sea. Journal of Foraminiferal Research 38:318–336.

Pope, K. O., K. H. Baines, A. C. Ocampo, and B. A. Ivanov. 1997. Energy, volatile production, and climatic effects of the Chicxulub Cretaceous/Tertiary impact. Journal of Geophysical Research 102:21.

Premovic, P. I., B. Z. Todorovic, and M. N. Stankovic. 2008. Cretaceous–Paleogene boundary (KPB) Fish Clay at Højerup (Stevns Klint, Denmark): Ni, Co, and Zn of the black marl. Geologica Acta 6:369–382.

Punekar, J., P. Mateo, and G. Keller. 2014. Effects of Deccan volcanism on paleoenvironment and planktic foraminifera: a global survey. Geological Society of America Special Paper 505:91–116.

Punekar, J., G. Keller, H. M. Khozyem, T. Adatte, E. Font, and J. Spangnberg. 2016. A multi-proxy approach to decode the end-Cretaceous mass extinction. Palaeogeography, Palaeoclimatology, Palaeoecology 441:116–136.

Quillévéré, F., R. D. Norris, D. Kroon, and P. A. Wilson. 2008. Transient ocean warming and shifts in carbon reservoirs during the early Danian. Earth and Planetary Science Letters 265:600–615.

Richards, M. A., W. Alvarez, S. Self, L. Karlstrom, P. R. Renne, M. Manga, C. J. Sprain, J. Smit, L. Vanderkluysen, and S. A. Gibson. 2015. Triggering of the largest Deccan eruptions by the Chicxulub impact. Geological Society of American Bulletin 127:1507–1520.

Robin, E., D. Boclet, Ph. Bonte, L. Froget, C. Jehanno, and R. Rocchia. 1991. The stratigraphic distribution of Ni-rich spinels in

https://doi.org/10.1017/pab.2018.16 Published online by Cambridge University Press

Cretaceous–Tertiary boundary rocks at El Kef (Tunisia), Caravaca (Spain) and Hole 761C (Leg 122). Earth and Planetary Science Letters 107:715–721.

Röhl, U., J. G. Ogg, T. L. Geib, and G. Wefer. 2001. Astronomical calibration of the Danian time scale. *In* D. Kroon, R. D. Norris, and A. Klaus, eds. Western North Atlantic Paleogene and Cretaceous palaeoceanography. Geological Society of London Special Publication 183:163–183.

Samir, A. M., and A. B. El Din. 2001. Benthic foraminiferal assemblages and morphological abnormalities as pollution proxies in two Egyptian bays. Marine Micropaleontology 41:193–127.

Schoene, B., K. M. Samperton, M. P. Eddy, G. Keller, T. Adatte, S. A. Bowring, S. F. R. Khadri, and B. Gerch. 2015. U-Pb geochronology of the Deccan Traps and relation to the end-Cretaceous mass extinction. Science 347:182–184.

Schueth, J. D., T. J. Bralower, S. Jiang, and M. E. Patzkowsky. 2015. The role of regional survivor incumbency in the evolutionary recovery of calcareous nannoplankton from the Cretaceous/Paleogene (K/Pg) mass extinction. Paleobiology 41:1–19.

Schulte, P., L. Alegret, I. Arenillas, J. A. Arz, P. J. Barton, P. R. Bown, T. J. Bralower, G. L. Christeson, P. Claeys, C. S. Cockell, G. S. Collins, A. Deutsch, T. J. Goldin, K. Goto, J. M. Grajales-Nishimura, R. A. F. Grieve, S. P. S. Gulick, K. R. Johnson, W. Kiessling, C. Koeberl, D. A. Kring, K. G. MacLeod, T. Matsui, J. Melosh, A. Montanari, J. V. Morgan, C. R. Neal, D. J. Nichols, R. D. Norris, E. Pierazzo, G. Ravizza, M. Rebolledo-Vieyra, W. U. Reimold, E. Robin, T. Salge, R. P. Speijer, A. R. Sweet, J. Urrutia-Fucugauchi, V. Vajda, M. T. Whalen, and P. S. Willumsen. 2010. The Chicxulub asteroid impact and mass extinction at the Cretaceous–Paleogene boundary. Science 327:1214–1218.

Smit, J. 1982. Extinction and evolution of planktonic foraminifera after a major impact at the Cretaceous/Tertiary boundary. Geological Society of America Special Paper 190:329–352.

——. 1990. Meteorite impact, extinctions and the Cretaceous/Tertiary Boundary. Geologie en Mijnbouw 69:187–204.

——. 1999. The global stratigraphy of the Cretaceous–Tertiary Boundary impact ejecta. Annual Review of Earth and Planetary Sciences 27:75–113.

——. 2004. The section of the Barranco del Gredero (Caravaca, SE Spain): a crucial section from the Cretaceous/Tertiary boundary impact extinction hypothesis. Journal of Iberian Geology 31:181–193.

Smit, J., and J. Hertogen. 1980. An extraterrestrial event at the Cretaceous–Tertiary boundary. Nature 285:198–200.

Smit, J., and A. J. T. Romein. 1985. A sequence of events across the Cretaceous–Tertiary boundary. Earth and Planetary Science Letters 74:155–170.

Smit, J., and W. G. H. Z. ten Kate. 1982. Trace-element patterns at the Cretaceous–Tertiary boundary—consequences of a large impact. Cretaceous Research 3:307–332.

Smit, J., T. B. Roep, W. Alvarez, A. Montanari, P. Claeys, J. M. Grajales-Nishimura, and J. Bermudez. 1996. Coarse-grained, clastic sandstone complex at the K/T boundary around the Gulf of México: deposition by tsunami waves induced by the Chicxulub impact? Geological Society of America Special Paper 307:151–182.

Stouff, V., J. P. Debenay, and M. Lesourd. 1999. Origin of double and multiple tests in benthic foraminifera: observations in laboratory cultures. Marine Micropaleontology 36:189–204.

Sujata, K. R., R. Nigam, R. Saraswat, and V. N. Linshy. 2011. Regeneration and abnormality in benthic foraminifera *Rosalina leei*: implications in reconstructing past salinity changes. Rivista Italiana di Paleontologia e Stratigrafia 117:189–196.

Thibault, N., B. Galbrum, S. Gardin, F. Minoletti, and L. Le Callonnec. 2016. The end-Cretaceous in the southwestern Tethys (Elles, Tunisia): orbital calibration of paleoenvironmental events before the mass extinction. International Journal of Earth Sciences (Geologische Rundschau) 105:771–795.

Toon, O., D. Morrison, R. P. Turco, and C. Covey. 1997. Environmental perturbations caused by the impacts of asteroids and comets. Reviews of Geophysics 35:41–78.

Tyszka, J. 2006. Morphospace of foraminiferal shells: results from the moving reference model. Lethaia 39:1–12.

Vellekoop, J., A. Sluijs, J. Smit, S. Schouten, J. W. H. Weijers, J. S. S. Damsté, and H. Brinkhuis. 2014. Rapid short-term cooling following the Chicxulub impact at the Cretaceous–Paleogene boundary. Proceedings of the National Academy of Sciences USA 111:7537–7541.

Vellekoop, J., J. Smit, B. van de Schootbrugge, J. W. H. Weijers, S. Galeotti, J. S. Sinninghe Damsté, and H. Brinkhuis. 2015. Palynological evidence for prolonged cooling along the Tunisian continental shelf following the K–Pg boundary impact. Palaeogeography, Palaeoclimatology, Palaeoecology 426:216–228.

Venturati, A. 2006). Twin and bilobated chambered Cretaceous planktonic foraminifera: abnormal forms induced by high paleoenvironmental stress? Pp. 25–29 in Proceedings of National Conference "Geosciences 2006," Sofia, Bulgaria.

Verga, D., and I. Premoli Silva. 2002. Early Cretaceous planktonic foraminifera from the Tethys: the genus *Leupoldina*. Cretaceous Research 23:189–212.

Wade, B. R., P. N. Pearson, W. A. Berggren, and H. Pälike. 2011. Review and revision of Cenozoic tropical planktonic foraminiferal biostratigraphy and calibration to the geomagnetic polarity and astronomical time scale. Earth-Science Reviews 104:111–142.

Weinkauf, M. F. G., T. Moller, M. C. Koch, and M. Kucera. 2014. Disruptive selection and bet-hedging in planktonic Foraminifera: shell morphology as predictor of extinctions. Frontiers in Ecology and Evolution 2:1–12.

Yanko, V., M. Ahmad, and M. Kaminski. 1998. Morphological deformities of benthic foraminiferal tests in response to pollution by heavy metals: implication for pollution monitoring. Journal of Foraminiferal Research 28:177–200.

https://doi.org/10.1017/pab.2018.16 Published online by Cambridge University Press